OPTIMIZATION OF A CMOS-MEMS RESONATOR FOR APPLICATIONS OF RELATIVE HUMIDITY MEASUREMENT

MOHAMED AHMED ELTAYEB FADLALLA

ELECTRICAL AND ELECTRONIC ENGINEERING

UNIVERSITI TEKNOLOGI PETRONAS

JANUARY 2017

Optimization of a CMOS-MEMS Resonator for Applications of Relative Humidity Measurement

By

MOHAMED AHMED ELTAYEB FADLALLA

17766

Dissertation Submitted

In Partial Fulfillment of the Requirements for the

Bachelor of Engineering (Hons)

(Electrical & Electronic Engineering)

January 2017

Universiti Teknologi PETRONAS
Bandar Seri Iskandar
31750 Tronoh
Perak Darul Ridzu

This thesis is dedicated to the memory of my father, Ahmed Eltayeb Fadlalla. His love for family and thirst for knowledge continues to inspire me today.

CERTIFICATION OF APPROVAL

Optimization of a CMOS-MEMS Resonator for Applications of Relative Humidity Measurement

By

MOAHMED AHMED ELTAYEB FADLALLA

17766

A project dissertation submitted to the
Electrical and Electronic Engineering Programme
Universiti Teknologi PETRONAS
in partial fulfilment of the requirement for the
BACHELOR OF ENGINEERING (Hons)
(ELECTRICAL AND ELECTRONIC ENGINEERING)

Approved by,

_____

Dr. Abdelaziz Yousif Ahmed Almahi

UNIVERSITI TEKNOLOGI PETRONAS
TRONOH, PERAK
January 2017

CERTIFICATION OF ORIGINALITY

This is to certify that I am responsible for the work submitted in this project, that the original work is my own except as specified in the references and acknowledgements, and that the original work contained herein have not been undertaken or done by unspecified sources or persons.

_____

Mohamed Ahmed Eltayeb Fadlalla

Abstract

The mathematical modeling and the finite element analysis (FEA) of a Complementary Metal Oxide Semiconductor-Microelectromechanical System (CMOS-MEMS) resonator has been presented. The resonator is designed based on 0.35 μm CMOS foundry fabrication technology. The sensing principle of the resonator is based on the change in resonance frequency of the CMOS-MEMS resonator due to adsorption/absorption or desorption of humidity on the active material layer of deposited on the moving plate that results in changes in the mass of the device. Simple analytical models of the CMOS-MEMS resonator are generated to achieve estimates of the device performs. The effect of changes in lengths and widths of the beams on spring constant, resonance frequency, damping coefficient and quality factor (Q) are investigated. The spring constant is found to decrease with increase the lengths of the beam and increasing with increase the widths of the beam. On the other hand, resonance frequency is found to decrease with increases in the lengths of the beam and increases with increase the widths of the beam. Further, the effect of air damping is investigated and found to decreases from 194×10^{-9} Ns/m to 7.2×10^{-9} Ns/m with increase in the air gap distance between the resonator and substrate from 100 μm to 300 μm. The *Q* factor of the CMOS-MEMS resonator is found to decrease with increasing damping coefficient, while the frequency remained unaffected. Finally, FEA simulation using 2008 CoventorWare software was used to confirm the modelled results, in which the modelled and simulated frequencies was found to be close within a percentage error from 1.1% to 4.47%.

Acknowledgment

First and foremost, all praise to Allah for his blessings, I would like to express my sincere gratitude towards my supervisor Dr. Abdelaziz Yousif Ahmed Almahi for his expert guidance and continuous support throughout the course of my final year project. In addition to being an excellent supervisor, he always lent me a helping hand when required and I deeply appreciate it.

Special thanks to my co-supervisor AP. Dr. John Ojur Dennis for his help in overcoming and troubleshooting the problems faced throughout the project, and as my GA Mr Almur Abdelkreem.

My deepest gratitude to the Universiti Teknologi PETRONAS, for providing the highest standards of education and guiding future generations to be of significance to society. May the light of your teaching shine for many generations to come.

To my family, for their endless support throughout every step of my life I am eternally grateful. My parents and my siblings have always been there for me and have helped me develop as an individual. All of the fond memories I have had with my friends will linger for many years to come, and I would like to thank everyone who contributed in any way possible, towards the success of this project.

Table of Contents

List of Figures

List of Tables

Chapter 1

Introduction

1.1 Background

In order to apprehend the concept of humidity, we must realize that there is water in the air surrounding us. Furthermore, that water is in a form of gas, which is called water vapor. Humidity can be defined as the amount of water vapor surrounding us. However, there are two different terms of humidity, which they are Absolute Humidity and Relative Humidity. The term absolute humidity is used for the mass of water vapor divided by the mass of dry air in a certain volume of air at a specific temperature. On the other hand, relative humidity is the ratio of the current absolute humidity to the highest possible absolute humidity, which depends on that specific temperature.

Sensors are devices that operate by detecting and responding to certain type of inputs and outputs from the surrounding physical environment. Furthermore, the input can vary from motion, heat, light, pressure or any other environmental phenomena. In addition, the output is usually a signal which is altered to a readable display [1]. Nowadays, sensors are used for their low cost, small size, easy integration into systems, low power consumption, and high performance. The improvement of sensors was initiated by various number of technologies such as: Piezo-materials, Micro-machines and other handful technologies. For the last few decades, humidity sensors have become a real interest, with applications in countless medical fields, industrial fields and many other critical applications.

Complementary Metal Oxide Semiconductor (CMOS) technology has become unquestionably the leading fabrication technology for integrated circuits (ICs) over the last decades. Currently, a variation of Microsensors and Microelectromechanical Systems (MEMS) are also exploiting the benefits of CMOS technology [2].Moreover, within the regular CMOS process there are several classes of MEMS can be utterly made such as optical, magnetic and temperature sensors [3]. Further, CMOS-MEMS Resonator is one of the main foundations of decreasing the power consumption and the cost for so many applications. Oscillator circuits in timing applications and sensory are the main

applications for the COMS-MEMS Resonators. It is safe to say that the key element for controlling frequency is Mechanical Resonators [4]

1.2 Problem Statement.

Efficiency is considered as one of the most important challenges in the sensing technology. Further, the efficiency of humidity sensors is driven by several number of parameters, these parameters are power consumption, response time, hysteresis and sensitivity [5]. Nowadays, Capacitive and Resistive humidity sensors are the most common sensors in the market. However, these two types of sensors have quite a few number of drawbacks, one of these drawbacks is hysteresis [6]. Furthermore, hysteresis means that the current state of the system still depends on its history, so in case of humidity sensors, the adsorption curve doesn't match the desorption curve [7]. Moreover, reversibility is also one of the drawbacks of resistive and capacitive humidity sensors, which occurs during the detection process. The absorbed water vapor will stick on the top of the sensing material, which affects the sensitivity and the efficiency of the sensor. Based on Dennis, et al. [8], these two drawbacks were resolved on the first generation of a CMOS-MEMS Mass-sensitive Relative Humidity Sensor. The device showed very promising results, which gives us the opportunity for further investigations and optimizing a second generation from the device.

1.3 Objectives and Scope of the Study.

The main objective of this research is to optimize the CMOS-MEMS resonator for applications of relative humidity measurement for high sensitivity and low stiffness. The specific objectives of the study are:

- To optimize the existing CMOS-MEMS mass-sensitive relative humidity sensor fabricated in our previous research to enhance its response to relative humidity in the ambient environment.
- To optimize the device via finite element analysis (FEA) CoventorWare simulation software and validate the simulation results with appropriate mathematical modeling.

Chapter 2

Literature Review

2.1 Humidity Sensors

A Humidity sensor, is a sensor that responds to the presence of chemical quantities from the surrounding environment. Over the years, the influence of humidity over the human health has attracted many researchers [9, 10]. Moreover, humidity sensors have become vital in daily life basis, with applications in air quality control and improvement, agriculture, pharmaceutical processing, industry production, weather forecasting, green houses, health assessment devices, etc. [11, 12]. Wolkoff and Kjærgaard [13] stated that low relative humidity (below 30% RH) irritates both the upper air and the eyes and cause nose and throat dryness. While, Arundel, et al. [14] reported that the severity of asthma has been reduced with higher levels of relative humidity. Humidity sensors can be categorized based on the sensing principle used. In addition, there are various types of humidity sensors such as, capacitive, resistive, mass detection, mechanical, thermo-elemental, and many others [5, 11, 15].

2.1.1 Traditional Capacitive and Resistive Humidity Sensors

Capacitive humidity sensors are commonly used in green houses, weather telemetry, commercial and industrial applications. A capacitive humidity sensor consists of substrate, thin or thick film, of the sensing material and two conductive electrodes. The sensing principle is based on changing in the dielectric constant of the sensing materials due to the humidity level of the surrounding environment. The basic structure of capacitive humidity sensor consists of alumina substrate, base electrode, connection terminal, upper electrode, lower electrode and polymer sensitive material as shown in Figure (1) [16].

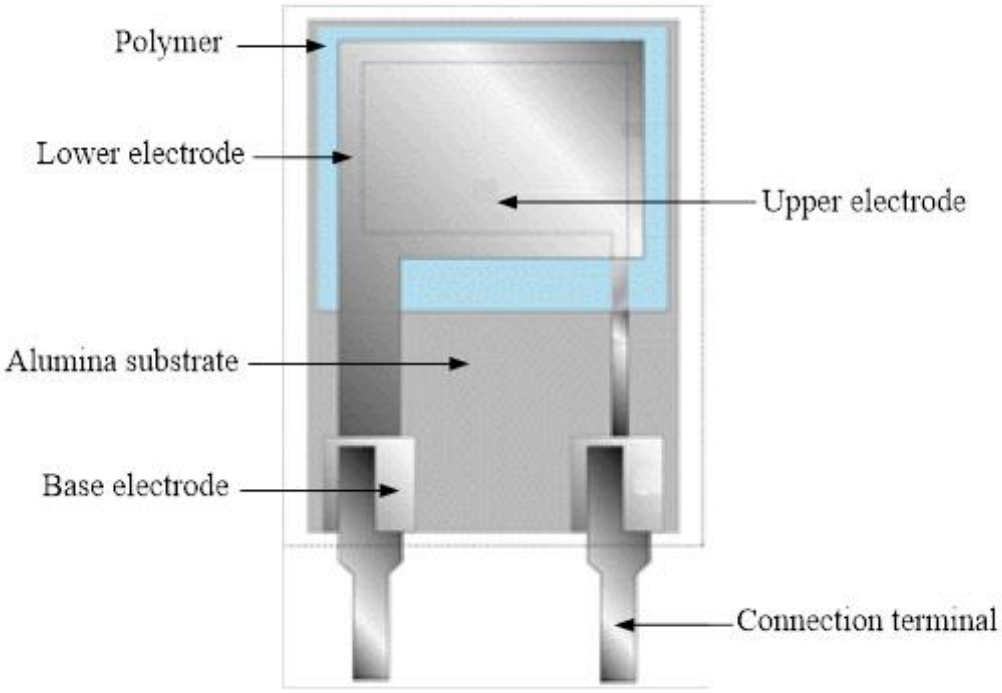

Figure 1 Capacitive humidity sensor [16]

The sensing principle of resistive humidity sensor is based on changes in the resistance value of the sensor due to absorption/adsorption of humidity onto sensing material. The basic structure of resistive humidity sensor consists of alumina substrate, base electrode, connection terminal, comb electrode and polymer sensitive material as shown in Figure (2). In 2010, Yoo, et al. [17] reported about the fabrication of a novel resistive-type relative humidity sensor. The sensitivity of the device is found to be about 0.0047 /% RH.

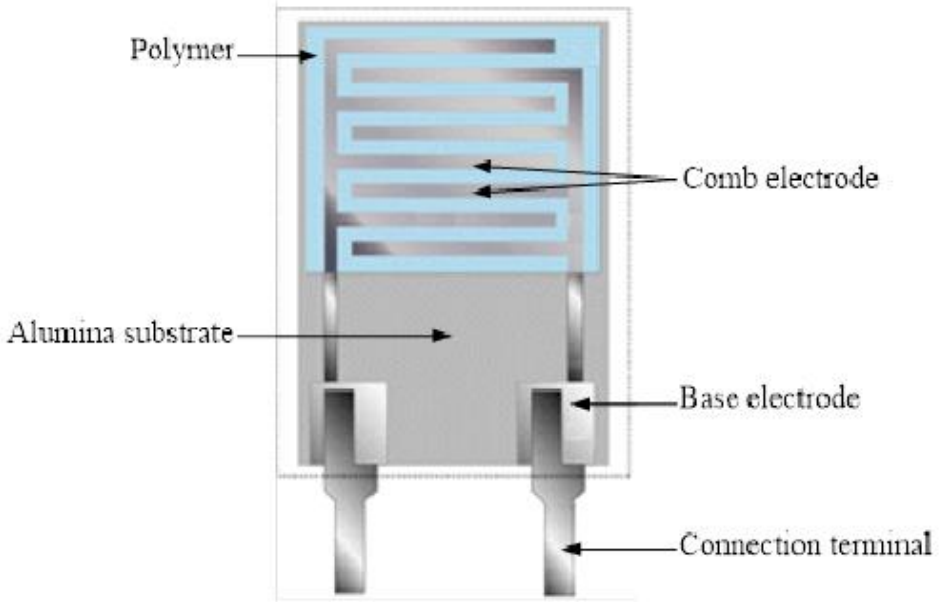

Figure 2 Resistive humidity sensor [16]

Nowadays, capacitive and resistive are the most common types of humidity sensors in the market. However, these two types of humidity sensors have revealed that the hysteresis of the sensors are quite high. Furthermore, Gu, et al. [18] stated that a capacitive humidity sensor with maximum hysteresis of 3% at 80% relative humidity. Figure (3) illustrate the hysteresis graph of the sensor. On the other hand, Su and Uen [19] stated that a resistive humidity sensor showed a hysteresis within 5.9% relative humidity. Figure (4) illustrate the hysteresis graph for the resistive humidity sensor.

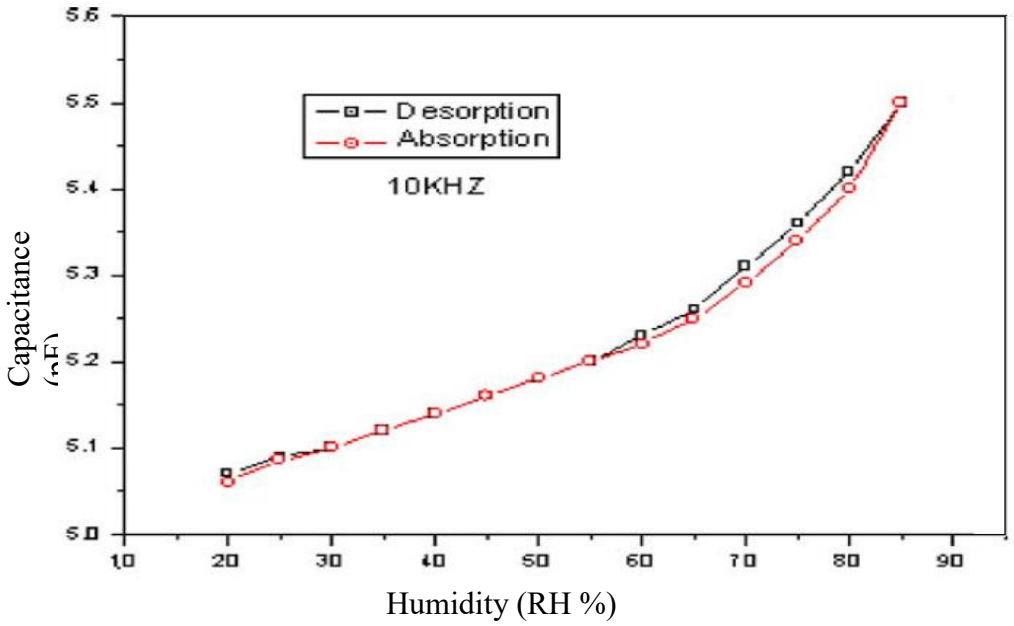

Figure 3 Hysteresis graph for a capacitive humidity sensor [18]

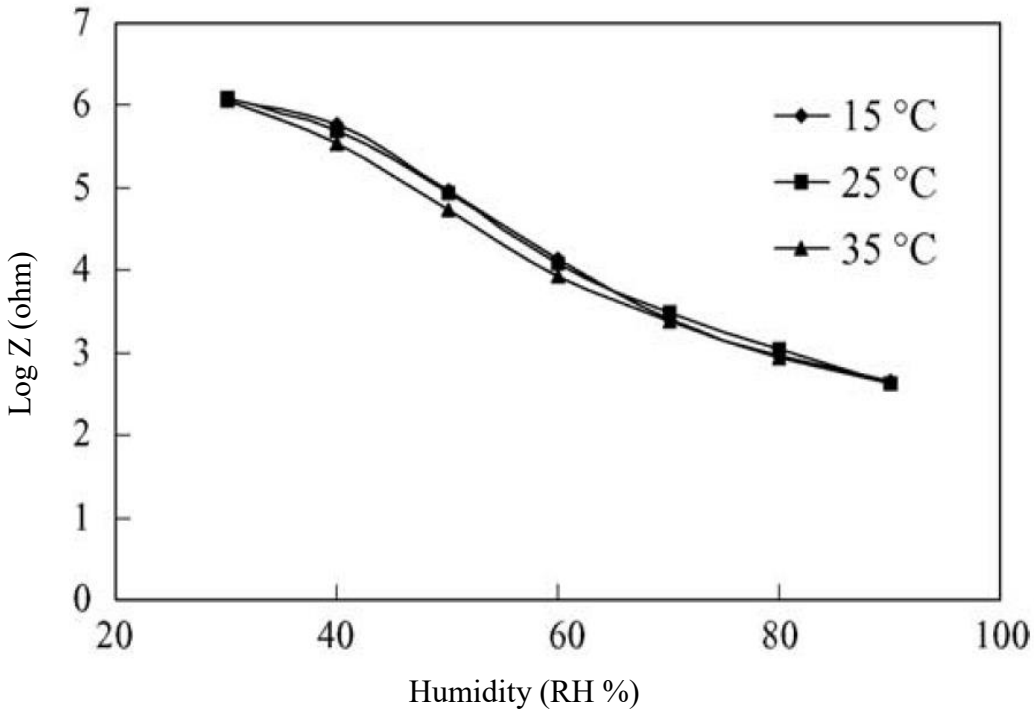

Figure 4 Hysteresis graph for a resistive humidity sensor [19]

2.2 The Integration between CMOS-MEMS.

The attempt of using the standard CMOS materials for the fabrication of MEMS instead of the materials traditionally used in poly-silicon-based MEMS was encouraged by many researchers recently. The integration of CMOS-MEMS can be achieved during the interconnection of the CMOS circuits on one part of the wafer, while forming a complex MEMS by using the metallic materials and patterned layers on another part of the wafer [20]. CMOS technology impedes minimization of the electronic and the cost-down due to its incompatibility, while the integration with MEMS technology mainly offers an enhanced signal transduction, enhanced immunity from the electromagnetic interference, low power consumption and small chip size [4, 21].

A resonator is a device that is designed to reveal a resonant behavior that is, it naturally oscillates at some frequencies. MEMS resonators are well known as a very promising technique for mass detection. MEMS resonators offer a high *Q* factor, stability and satisfactory power handling capability [22]. A piezoresistive transducer is used in order to transduce the resonant motion into an electrical signal. CMOS-MEMS resonators are supported by a number of beams, each beam has a piezoresistor that is placed at the tip of the beam. The piezoresistors are placed at the tip due to stress, which is the maximum at that point. Based on resonance change physical, chemical and biological changes are detected, which makes resonance tuning essential to several resonant sensors [23, 24].

MEMS technology is very suitable as a platform to produce micro-machined sensors or actuators. An actuator device can be defined as a device that convert an input energy to a mechanical energy [25]. According to different forms of input energy, several number of actuators were developed and put into practical use. It can be said that, collecting and connecting the analog information to the digital world is the main function of sensors and actuators. Sensors and actuators interact directly with their surrounding environment which is dissimilar with IC's, and usually they have moving part [26]. MEMS technology offers four major classes of actuators, which they are Electrostatic, Magnetic, Piezoelectric and Electrothermal actuations.

2.3 Sensing techniques

Nowadays, sensors are considered as a crucial component of a system. A Sensor is a device that is used to measure, detect, indicate, record or otherwise react to the received information. Hence, the main task of a sensor is to convert the received stimulus into a measured signal [27]. Further, there are many types of stimulus such as thermal, mechanical, electromagnetic or chemical in origin (and so on) [28]. MEMS sensors are used to measure various kinematics such as acceleration, impact, vibration, force, torque, stress, strain and displacement. However, sensing techniques are based on the sensing principle of a sensor. In addition, there are different types of sensing principle, some of which are: electromagnetic, piezoelectric, capacitive, piezoresistive.

2.3.1 Capacitive Sensing.

MEMS capacitive sensors are usually used as a position sensor, which is employed in nan-positioning application in order to develop a high precision angular and X-Y linear position sensor [29]. Furthermore, capacitive sensors has the capability of sensing a large range of movements at high speed. Lastly, capacitive sensors offer both high resolution capability at low cost, and an easy fabrication process.

2.3.2 Piezoresistive sensing.

In recent times, using Piezoresistance technique as a transducer has become the most employed technique in MEMS technology [27]. In 1954, the effect of piezoresistor in semiconductor was first discovered in both Silicon (Si) and Germanium (Ge) by smith [30]. Furthermore, the detection process of a piezoresistive sensor is based on the change in the electrical resistance of the Piezoresistor material due to the applied mechanical strain. Furthermore, the gauge factor of a Piezoresistor can be repressed by several factors such as, doping level, grain size, temperature, etc, [31]. Moreover, it has been discovered that the piezoresistive transduction has an enhanced performance to other sensing transducers [32]. In addition, as result of the temperature effect in piezoresistive devices, the applications of these devices were limited. Further, piezoresistors are usually fabricated by using polycrystalline silicon films, which is also referred to as poly or polysilicon. In 1970s and 1980s, a comprehensively studies on the piezoresistive effect were conducted [33, 34].

2.4 MEMS Actuation Methods

To operate the CMOS-MEMS devices in vibration (dynamic mode), it is necessary for the devices to be vibrating by converting the electrical energy to mechanical motion and there are several different types of MEMS actuation methods such as electrostatic, electromagnetic, piezoelectric and electrothermal.

2.4.1 Electrostatic Actuation Method

Electrostatic is the attraction between the oppositely charged conductors. Recently, electrostatically actuated MEMS are widely used for a various number of application such as sensors switches and resonators. In addition, an electrothermal actuator consists of at least two electrodes spaced from each other. Due to the electrostatic attraction, applying a direct current (DC) voltage between the two electrodes will result in the deflection of the deformable electrode towards to the fixed electrode. The advantages of a having an electrostatic actuated MEMS are low power consumption, small volume and fast response [26].

2.4.2 Electromagnetic Actuation Method

Magnetic actuation is the displacement because of the interaction between various magnetic elements, such as magnetizable material, current carrying wire or external magnet. Further, magnetic actuated MEMS offer plenty of benefits over the electrostatic actuation [35].

2.4.3 Piezoelectric Actuation Method

Piezoelectric actuation is the displacement due to strain which is induced by an electrical field. Additionally, piezoelectric devices do not require any Direct Current (DC) voltage for their operation. Using piezoelectric material gives the benefit of converting an electrical input into a mechanical output and vise-versa, due to the property of electromechanical coupling [36]. Various number of features are owned by piezoelectric actuators such as short response time, compact size, high output force and low power consumption. In addition, piezoelectric materials can be used for both actuation and sensing at the same time.

2.4.4 Electrothermal Actuation Method

Electrothermal Actuation can be defined as the displacement due to the thermal expansion. Lately, electro thermal actuation has been rising attention due to its unique advantages such as low actuation voltage, wide frequency tuning, high *Q*-factor and simple fabrication process [37]. The principle of operation for electrothermal actuation is by using the thermal expansion of a material as a driving force. Based on Joule heating and thereby thermal expansion of material, electrothermal actuation is considered as a transduction mechanism. Furthermore, electrothermal actuation has the ability to deliver a large displacements at a lower voltage. In addition, the electrical sensing of a mechanical vibration is a necessity for a MEMS resonator. An integration between electrothermal actuation and piezoelectric sensing has been presented lately to accomplish an effective actuation and sensing. As a result of the device is being electrothermally driven into resonance, the beam will start to vibrate, which will induce a mechanical strain in the top piezoelectric material. That process will result an alternating voltage with a frequency equal to the frequency of the resonator [37, 38]. The advantages and the disadvantages of each method are mentioned in Table (1).

Table 1 Advantages and disadvantages mems actuation methods

Actuation Method	Advantages	Disadvantages
Electrostatic	- Ability to sense as well as actuate - Ease to fabricate - Simplicity of materials - Fast actuation response	- High voltage - Low force - High power dissipation
Electromagnetic	- High force - Ability to sense as well as actuate	- High power dissipation - It not compatible with COMS fabrication - Difficulty to form on-chip
Piezoelectric	- High force - Low power dissipation. - Ability to be fabricated on the same chip	- Low output voltage - High impedance
Electrothermal	- High force - Lower actuation voltage - Large displacement - Fast actuation response	- Higher power dissipation - Sensitivity to environmental temperature changes

2.5 COMS-MEMS Humidity Sensor

Recent studies have employed the use of the commercial CMOS process in the fabrication of micro devices such as, gas sensors and humidity sensors. However, Chung, et al. [39] presented a capacitive humidity sensor based on the integration of CMOS-MEMS technology. In addition, the device was designed based on 0.18 µm CMOS process with one polysilicon and six metal layers. Further, the vertical parallel plates were combined with integrated mesoporous RF-aerogels as a moisture sensitive film. The device has shown a hysteresis of 1.1% RH. 30°C during absorption and desorption cycle, which is shown in Figure (5). In contrast, Dai [40] reported another capacitive CMOS-MEMS humidity sensor with a ring oscillator circuit. The device was fabricated using 0.35 µm CMOS process with a micro-heater. The working principle of the sensor is by changing the capacitance of the sensor into an oscillation frequency output. The sensor has experienced with a very low hysteresis that is shown in Figure (6).

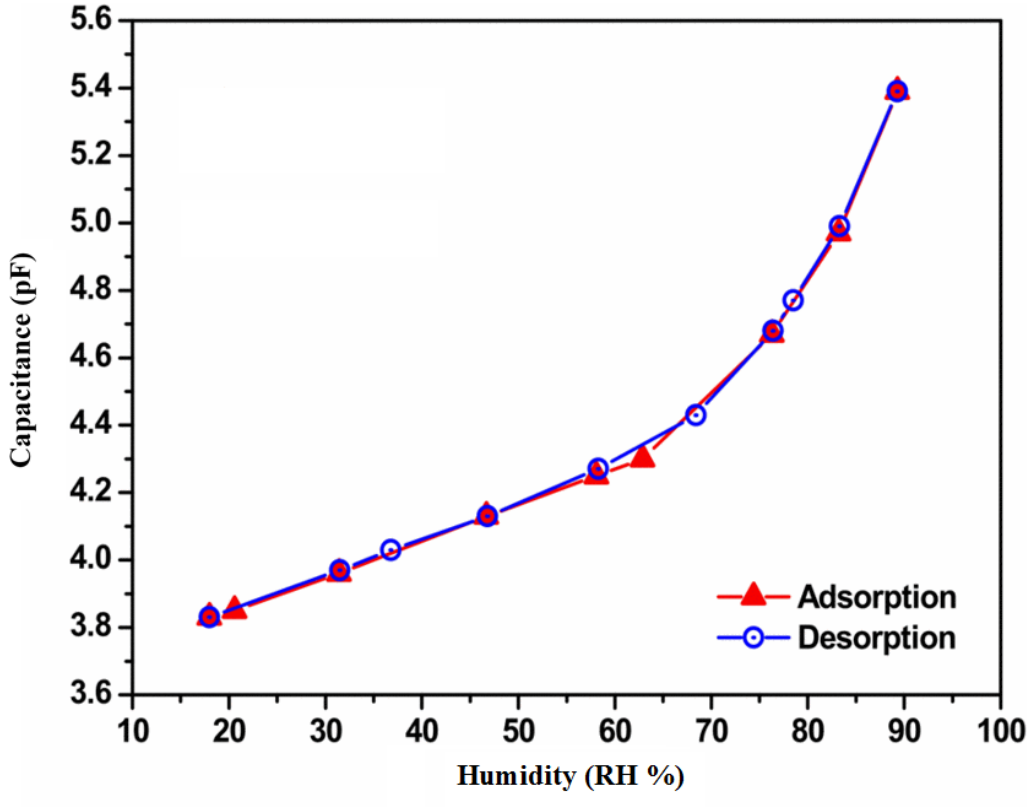

Figure 5 Hysteresis graph for a CMOS-MEMS humidity sensor [39]

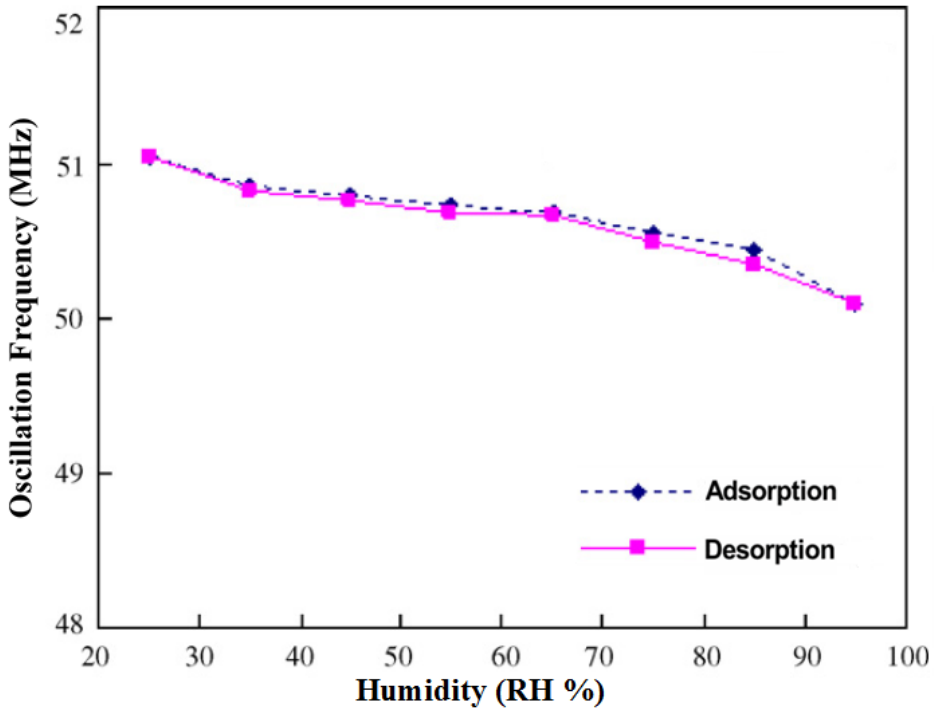

Figure 6 Hysteresis graph for a CMOS-MEMS humidity sensor [40]

Dennis, et al. [8] reported that a humidity sensor was fabricated in Universiti Teknologi PETRONAS for the purpose of measuring relative humidity using (CMOS-MEMS Resonator) technology. Furthermore, a micro-heater that operates at high temperature was used in the sensor to overcome the problem of reversibility. The fabricated sensor was enhanced with a temperature sensor that was placed on the top of the micro-heater. Further, the purpose of the temperature sensor was only used to monitor the temperature measurements within the device and the piezoresistive that is responsible for sensing the change in the output voltage. This device is operating by using mass detection method and it is actuated through electrothermal actuation, while the piezoresistive materials were used for sensing purposes. Furthermore, the sensor generally use the principle of mass detection, by detecting the changes in the resonant frequency of the resonator due to the mass change. The device was successfully fabricated and it has shown a very promising results, with hysteresis of 0.87% relative humidity at 80% relative humidity. Figure (7) illustrates a Field Emission Scanning Electron Microscope (FESEM) image of the back sided of the CMOS-MEMS device, and front sideTiO_2 paste deposited on its plate. While,

Figure (8) illustrate the output graph of the sensor at 80°C with 6 Vpp applied voltage at 4Hz frequency.

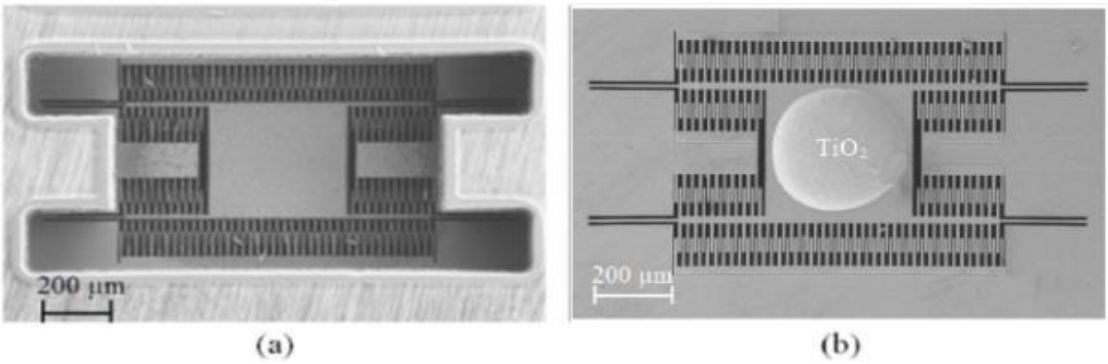

Figure 7 FESEM image of the device from (a) back side; (b) front sideTiO2 paste deposited on its plate [8]

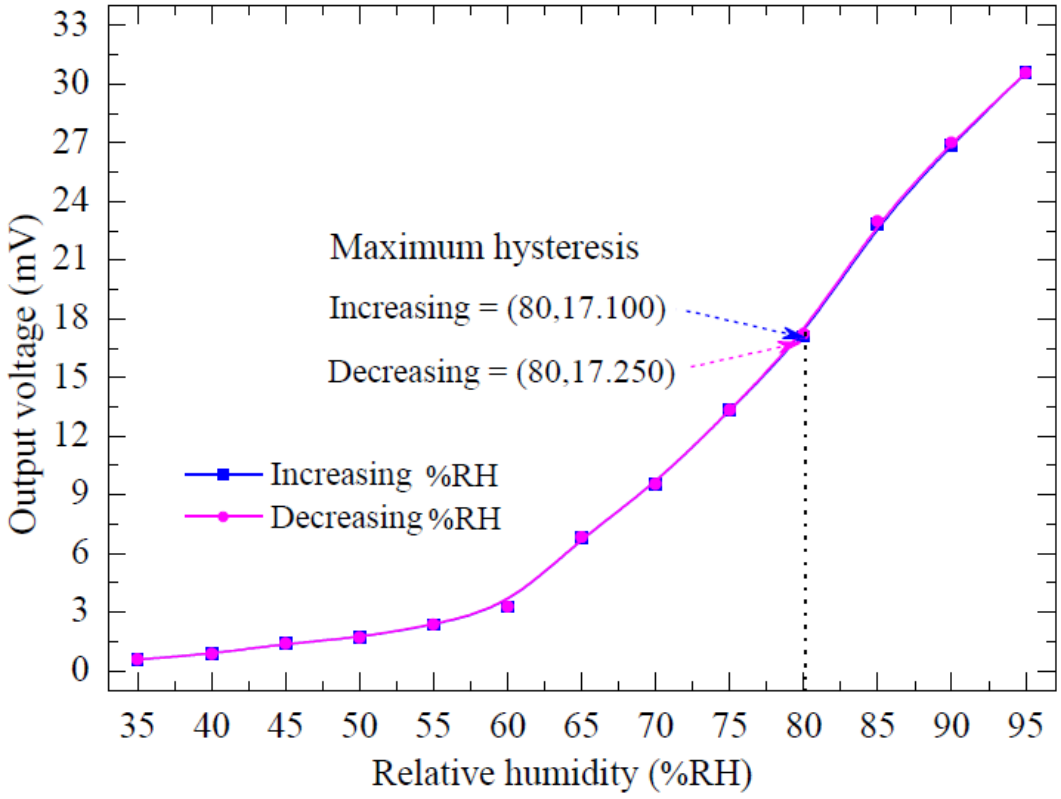

Figure 8 Output voltage of the humidity sensor vs. relative humidity [8]

Chapter 3

Methodology

This chapter presents the design, modeling, and simulation based on 0.35 µm CMOS fabrication technology and post-CMOS micromachining process steps of the CMOS-MEMS resonator. The chapter is divided into four sections. Section 3.1 gives an overview of the research methodology and flow chart of the project. Section 3.2 and Section 3.3 describes the design parameters and mathematical modeling. While, Section 3.4 discuss the CoventorWare Simulation Software. Lastly, section 3.5 summarizes the chapter.

3.1 Research Methodology of the Study and Flow Chart of the Project

The research methodology of the study consists of two major parts:

i. Design parameters and mathematical modeling of the CMOS-MEMS resonator by numerical. The mathematical modelling of the CMOS-MEMS resonator is the first most important study to understand the fundamental operation of the resonator by using appropriate principles from electromechanical vibrations and thermodynamics for the heat transfer. The effect of changes in parameters such as the resonator dimensions (width and length of the beams) on its characteristics such as the spring constant, resonant frequency, air damping (squeeze film damping), quality factor and sensitivity will be theoretically investigate.

ii. Optimize the CMOS-MEMS resonator via finite element analysis (FEA) CoventorWare simulation software. CoventorWare version 2008 is the finite element analysis (FEA) simulation software will be used to verify the device parameters such as resonant frequency and *Q* factor. CoventorWare is one of the most comprehensive suites of MEMS design and simulation tools in the industry. It acts as a design environment that reduces design risk, reduces manufacturing time and lowers development costs. CoventorWare supports both system level and physical design approaches. Figure (9) shows the flow chart of the research methodology that will be carried out in order to achieve the research objectives.

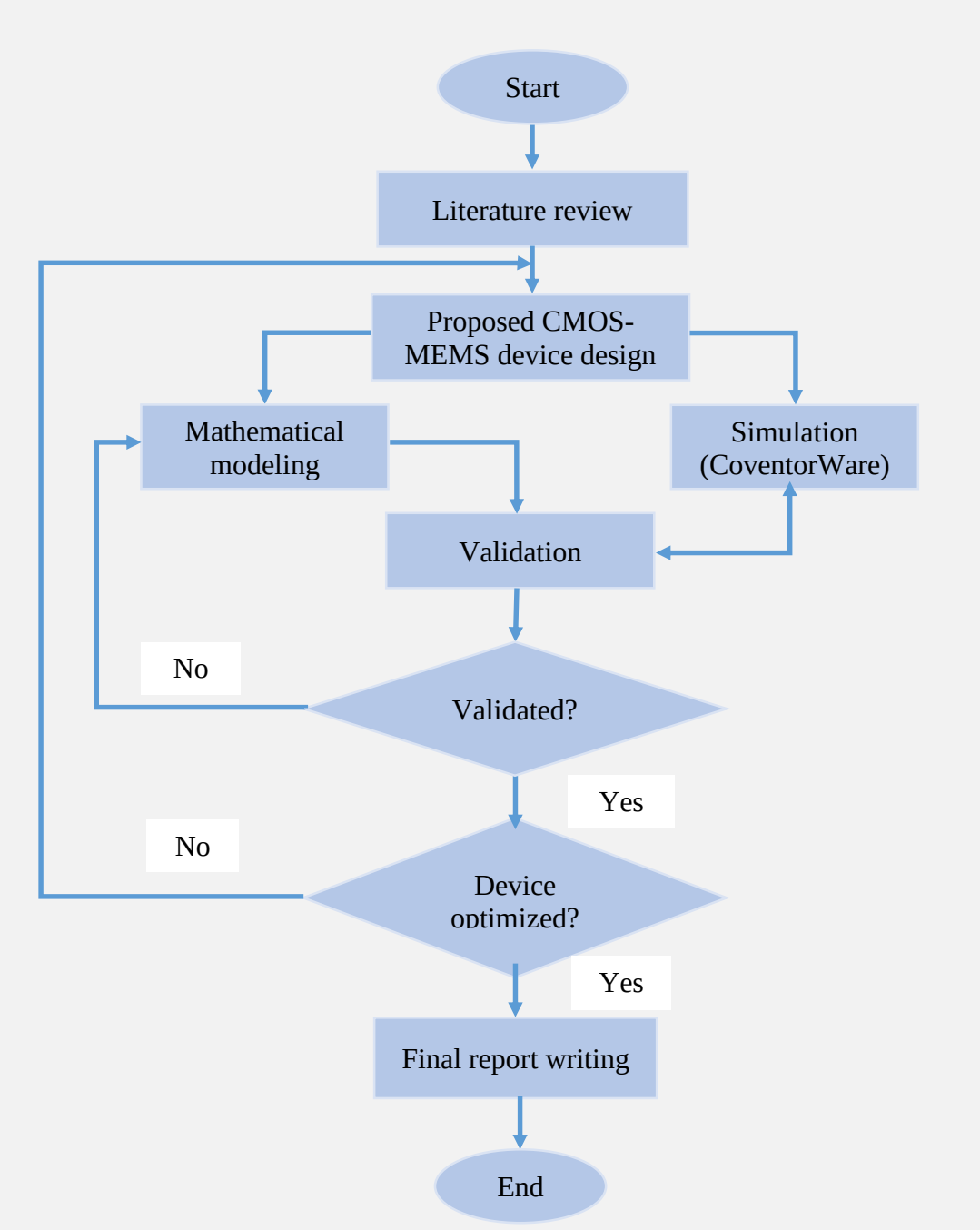

Figure 9 Project Flow Chart

Gantt chart carries the information of the project visually. Further, Gantt chart summarize all of the tasks of a project, and their order, shown against a timescale. This gives us an instant outline of a project, its related tasks, and when these tasks need to be completed. Table 2 represent the Gantt chart of the project during the period of FYP I, while Table 3 shows the plan for FYP II.

Table 2 Gantt chart For FYP I

Details/ Week	1	2	3	4	5	6	7	8	9	10	11	12	13	14
Topic Selection														
Literature Review														
Submission of extended proposal														
Mathematical modeling														
Proposal defiance														
Continuation of the project														
Submission of the interim draft report														

Table 3 Gantt chart For FYP II

Details/ Week	1	2	3	4	5	6	7	8	9	10	11	12	13	14	15
Continuation of the project															
CoventorWare simulation															
Results validation															
Submission of progress report															
Continuation of the project															
Pre-SEDEX															
Submission of Draft Final Report															
Submission of Dissertation (soft bound)															
Submission of Technical Paper															
Final viva															
Submission of Project Dissertation (Hard Bound)															

3.2 Design of the CMOS-MEMS Resonator

This project is intended for the optimization of the CMOS-MEMS Resonator for application of relative humidity in. furthermore, the schematic of the proposed design is illustrated in Figure (10). The device consists two plates, one is movable (rotor) and the other is fixed (stator). The dimensions of the plate are $400\ \mu m \times 400\ \mu m$, while the stator is anchored to the substrate. The fixed plate is supported by four beams, each beam has length (L) and width (W). The proposed design will be designed based on standard 0.35µm CMOS process. Table 4 shows the dimensions of the CMOS-MEMS Resonator.

Table 4 Dimensions of CMOS-MEMS Resonator

Parameter	Length (L)	Width (W)	Material (s)
Beam	300-500µm	10-18µm	M2, M3, SiO_2.
Micro-heater	6290µm	5µm	M1
Temperature Sensor	485µm	5µm	M1
Plate	400	400	M2, M3, SiO_2.

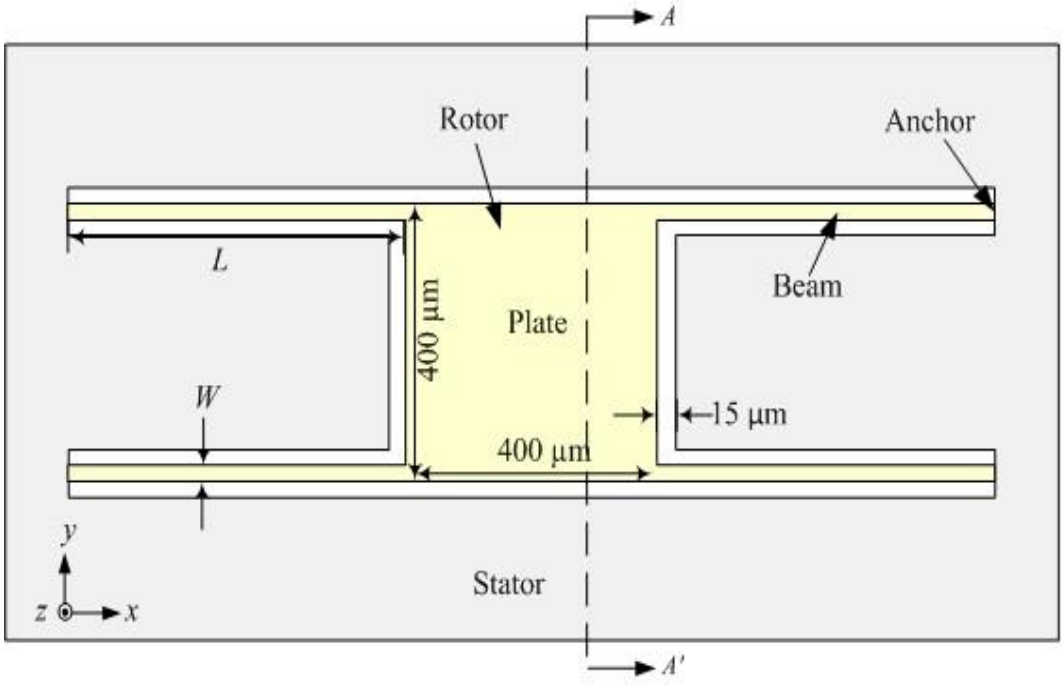

Figure 10 The schematic of the proposed design of the CMOS-MEMS Resonator

The CMOS process technology consists of one polysilicon layers, three metal, two vias and several dielectric layers. All metal layers are aluminum (Al), while, the dielectric layer and tungsten is made of silicon dioxide (SiO_2) which is used for the vias. The total thickness of the CMOS layers is 5 µm. Table 5 shows the typical thickness of the typical CMOS layers. The CMOS layers and the substrate are shown in Figure (11)**,** while the both of the young's modulus and the density of the CMOS layers are shown in Table 6.

Table 5 Typical thickness of the CMOS layers

Material	**Thickness**
Silicon dioxide under polysilicon	0.38 µm
polysilicon	0.285 µm
Silicon dioxide under metal 1	0.71 µm
Metal 1	0.624 µm
Silicon dioxide under metal 2	1 µm
Metal 2	0.612 µm
Silicon dioxide under metal 3	0.66 µm
Metal 3	0.877 µm

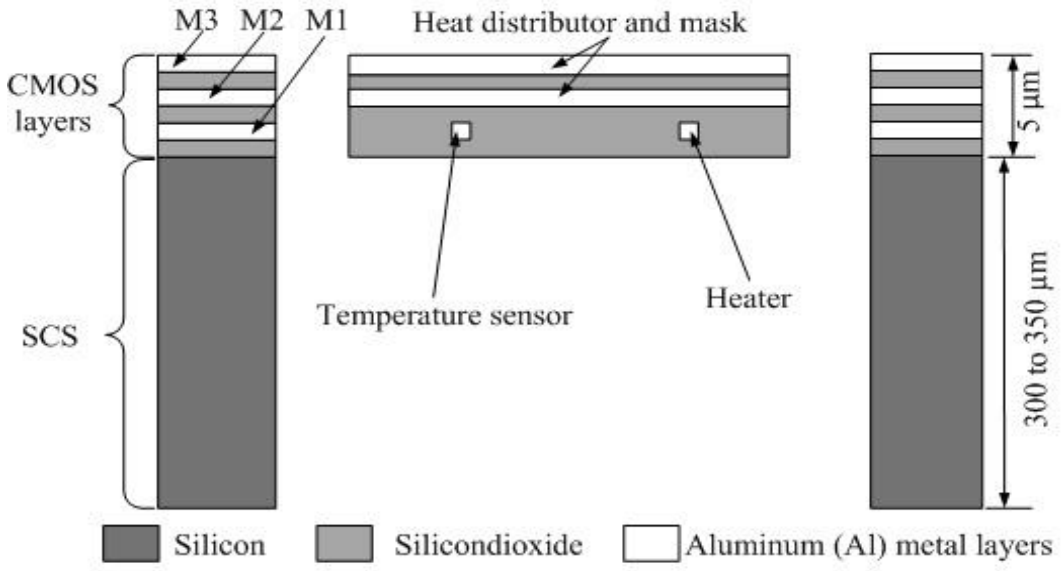

Figure 11 The CMOS layers and the single crystal silicon (SCS) substrate

Table 6 Young's modulus and density of the CMOS layers [33].

Properties	Silicon Dioxide (SiO_2)	Aluminum (Al)
Density (Kg/m)	2300	2700
Young's Modulus	72	70

Metal 1 (M1) will be used to form as the heating element and temperature sensor. Numerous approaches for the actuation of microelectromechanical system (MEMS) structures have been illustrated, these incorporate electrostatic, electromagnetic, piezoelectric and electrothermal. A heating element is used to actuate the device electrothermally as well as to operate the device at high temperature of 40 °C to 200 °C, with aim of improving its reversibility. The design chosen for the micro-heater is illustrated in Figure (12), with a meandering shape with length of 6290 µm and width of 5 µm, while the length of temperature sensor is 485µm. Lastly, M2 and M3 will be used as heat distributor to improve the uniformity of the temperature distribution

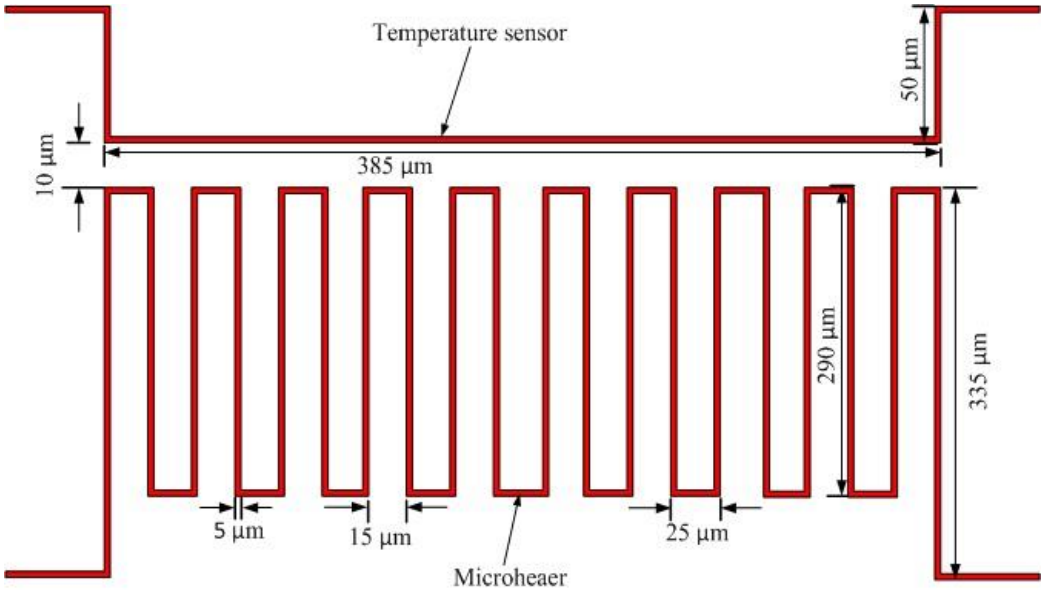

Figure 12 The design of the Micro-heater and the Temperature Sensor

3.3 Mathematical Modeling of the CMOS-MEMS Resonator

In this project, the mathematical modeling is used for further investigation on effects of the spring constant, resonant frequency and the damping coefficient. Furthermore, varying the length and the width of the beams of the proposed device has a significant effect on the physical behavior of the CMOS-MEMS resonator.

3.3.1 Electrothermal Actuation of the CMOS-MEMS Resonator

The CMOS-MEMS resonator will be using electrothermal actuation method to drive the resonator in the dynamic mode by applying sinusoidal alternating current (AC) $A_a\cos(wt)$ over the embedded micro-heater. This AC-current will produce temperature in the plate which translates into mechanical force and then make the device in vibratory motion due to difference in coefficient of thermal expansion. Furthermore, these vibrations will be producing stress at the anchor points of the supporting beams resulting a variation of the resistance of the piezoresistors (PZR) which can be measured using a Wheatstone bridge arrangement. Figure (13) shows schematic of electrothermal actuation of the CMOS-MEMS resonator with four polysilicon piezoresistors are placed at the anchor of the four sporting beams.

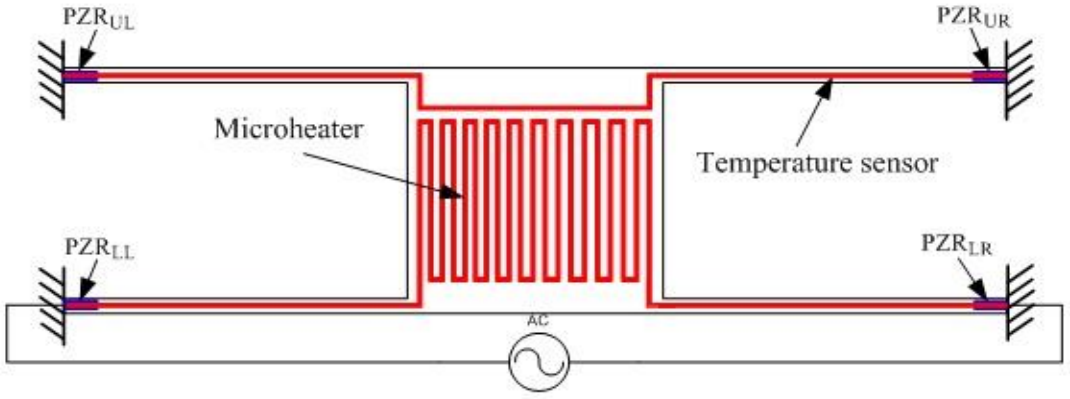

Figure 13 The schematic of electrothermal actuation of the CMOS-MEMS resonator with four polysilicon piezoresistors

3.3.2 Determination of Spring Constant, Resonance Frequency and Quality Factor.

In this project, the mathematical modeling of a CMOS-MEMS resonator is used to find the device parameters such as spring constant, resonance frequency and quality factor of the device. The device will be operating in out of plane oscillations in the *z* direction. Since the resonance frequency is subjected to the spring constant of the four beams which is given in Eq.(1) [41]

$$k = 4\frac{E_{av} w_b t^3}{l_b^3} \tag{1}$$

where w_b, l_b and t are the width, length, and thickness of the beams, respectively. E_{av} is the average young's modulus of the beams. The average young's modulus can be determined using Eq.(2) [42]

$$E_{av} = \frac{E_{Al} t_{Al} + E_{SiO2} t_{SiO2}}{t_{total}} \tag{2}$$

where E_{Al}, E_{SiO2}, t_{Al}, and t_{SiO2} are the young modules and thickness of aluminum and silicon dioxide, respectively. The effective mass of beam (m_{effb}) under bending moment is obtained using Eq.(3) [43]

$$m_{effb} = 4\frac{13}{35}\rho_{av} l_b w_b t \tag{3}$$

where ρ_{av} is average density of the CMOS layers, which can be estimated by using Eq.(4)

$$\rho_{av} = \frac{\rho_{SiO2} t_{Sio2} + \rho_{Al} t_{Al}}{t_{SiO2} t_{Al}} \tag{4}$$

where ρ_{SiO_2}, ρ_{Al}, t_{SiO_2} and t_{Al} are the densities and thicknesses of the SiO_2 and Al layers, respectively. The mass of plate (m_p) is given by Eq. (5) [44] and the total mass (m_{total}) of the device is the sum of the mass of plate and effective mass of the four beams is given by Eq.(6)

$$m_p = \rho_{av} l_p w_p t \tag{5}$$

$$m_{total} = \rho_{av} l_p w_p t + 4\frac{13}{35}\rho_{av} l_b w_b t \tag{6}$$

The general equation of resonance frequency is given by Eq. (7) [45]

$$f = \frac{1}{2\Pi}\sqrt{\frac{k}{m_{total}}} = \frac{1}{\prod}\sqrt{\frac{E_{av} w_b t_b^3}{\rho_{av} l_b^3\left(l_p w_p t_p + \frac{52}{35} l_b w_b t_b\right)}} \tag{7}$$

3.3.3 Air Damping Coefficient

Many MEMS devices are intended to operate in air and viscous fluids. However, in MEMS resonator the trapped air beneath the resonator will cause an interaction with the vibrating micro-plate [46]. For the resonance frequency to increase, the size of must be decreased. As result of that, the surface to volume ratio will be high, which means that the air damping will have a huge impact on micro resonator. Thus, it necessary to take under consideration the rarefaction effects of the air gap heights and the thin film. The damping ratio, which is the ratio of the actual damping coefficient (b_z) to the critical damping coefficient (b_c) is given by Eq. (8) [43], while critical damping coefficient (bc) is obtained Eq. (9)

$$\zeta = \frac{b_z}{b_c} \tag{8}$$

$$b_c = 2\sqrt{km} \tag{9}$$

The total damping coefficient (b_z) in *z* direction is expressed as squeeze film damping as given by Eq. (10) and the resonance frequency under the effect of damping is determined by Eq. (11)

$$b_{squeeze} = \eta\left[\frac{4 \times 0.422 l_b w_b^3 + 0.422 l_p^4}{x^3}\right] \tag{10}$$

where η is the dynamic viscosity of air, which is equal to 1.8×10^{-5} Pa.s ($N.s.m^{-2}$) at one atmospheric pressure and 20ºC [47] and *x* is the gap where the air is traped between the resonator and substrate

$$f_z = \frac{1}{2\Pi}\sqrt{\frac{k}{m_{total}} - \frac{b_z^2}{4m_{total}^2}} \tag{11}$$

The *Q* factor under the influence of damping can be determined by Eq. (12) [48]

$$Q_z = \frac{\sqrt{m_{total}k_z}}{b_z} \tag{12}$$

3.3.4 Design of Piezoresistor

Piezoresistive technique is employed in millions MEMS such as, accelerometer, flow sensor and pressure sensors. Further, the high sensitivity a single-crystal silicon was first discussed by Kanda [31] using a carrier transfer mechanism and the effective mass allied with *k*-space energy surface. The coefficient π- is used to describe the piezoresistivity of a material. Due to the symmetry of the silicon crystal only the coefficients are needed (π_{11}, π_{12}, π_{44}). The change ΔR in piezoresistor is can be calculated using Eq. (13) [49].

$$\Delta R = G\varepsilon R \tag{13}$$

where G is gauge factor piezoresistor, and depends on the direction of the applied stress, ε is the strain. While, a resistor R can be found using Eq. (14) [49].

$$R = \frac{\rho_r l_r}{w_r t_r} \tag{14}$$

where ρ_r is the resistivity of the material, is the l_r length if the resistor, w_r is the width of the resistor and t_r is the thickness of the resistor. As a function of applied strain, a fixed piezoresistor on a stressed beam go through transverse and longitudinal resistivity. The change of resistivity in longitudinal resistor can be obtained using Eq.(15) [49].

$$\left(\frac{\Delta\rho_r}{\rho_r}\right)_L = g_L\varepsilon_L \tag{15}$$

where g_L and ε_L are the longitudinal gauge factor and strain respectively. The relation between the longitudinal gauge factor and π-coefficient is expressed by Eq. (16) [49].

While, for randomly oriented polysilicon grains, the longitudinal Piezoresistance coefficient is given by Eq. (17) [49].

$$G_L = \pi_L E \tag{16}$$

$$\pi_L = \pi_{11} - 0.400\left(\pi_{11} - \pi_{12} - \pi_{44}\right) \tag{17}$$

3.4 CoventorWare Simulation Software

CoventorWare is a simulation software provided by Coventor for the purpose of offering a design methodology for microelectromechanical system (MEMS) devices and systems. CoventorWare software is considered as the core software used for the designing and the developing of MEMS devices. The software gives the ability to design in two contradictory ways, either from top down or bottom up. Furthermore, CoventorWare provides an easy to use and integrated design environment, which offers the most productive path for manufacturing MEMS devices. The software also allows the users to bypass computationally intensive tools during the initial design and research stages. CoventorWare has abundant MEMS features, which allows the user to:

- Rapidly explore and optimize design the process options.
- Develop MEMS devices at low Cost.
- Develop and produce MEMS devices with high efficiency.

CoventorWare is useful for MEMS experts and newcomers alike. Using CoventorWare, designers are guided to create a MEMS device quickly, then evaluate the MEMS device within the surrounding system to understand its behavior, environmental effects, and the effects of control circuitry. Furthermore, CoventorWare software consists of three major sections, each of these sections can be used either jointly to deliver a complete MEMS design flow, or independently to complement an existing design flow. The major CoventorWare's sections are: Architect, Designer and Analyzer. Figure (14) illustrates the CoventorWare typical design flow using only the designer and analyzer.

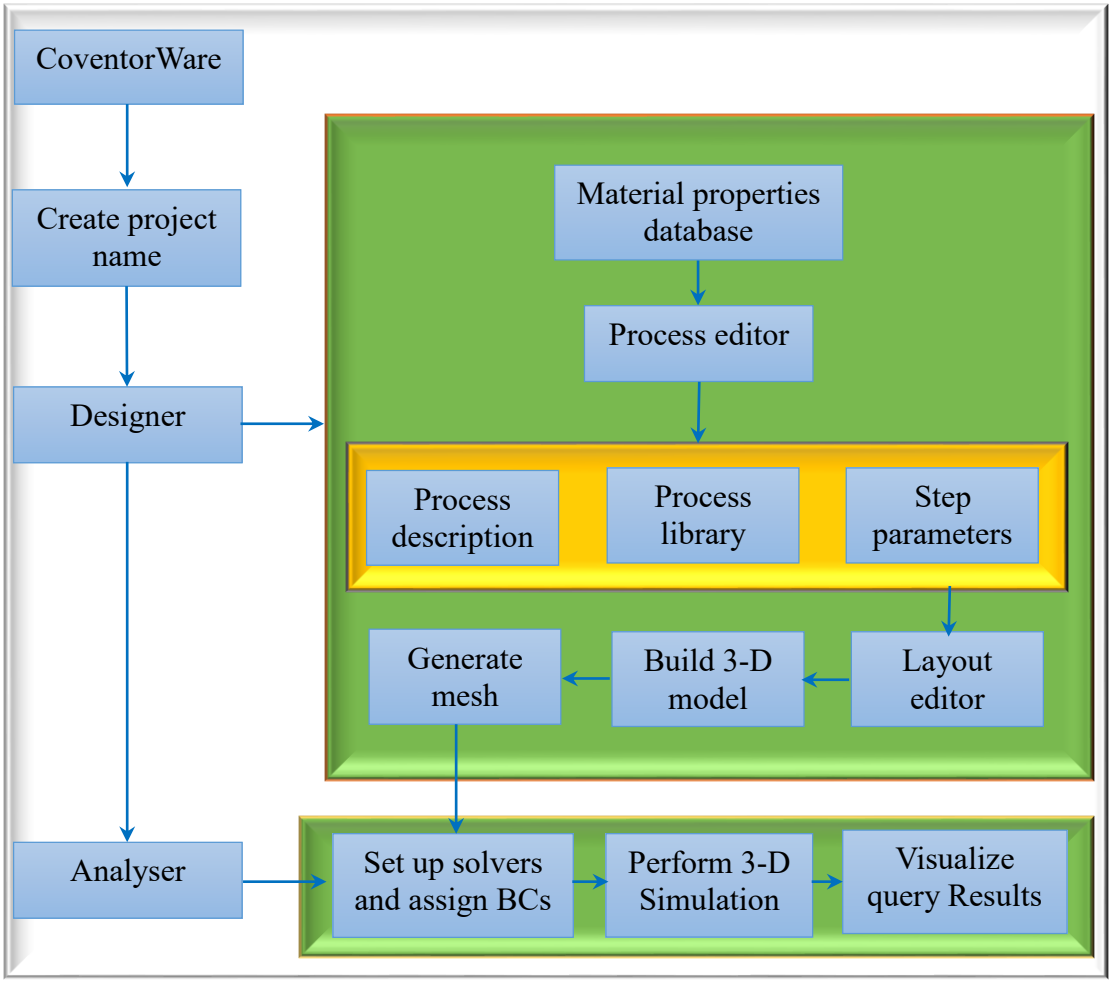

Figure 14 Typical design flow using both the designer and analyzer.

3.4.1 Architecture

The Architect offers a structured custom procedure driven design environment for top-down and simulation of MEMS devices and also the surroundings systems (Control circuits) of MEMS. Furthermore, the Architect is also known as the only simulation tool that quickly enough to evaluate the performance of MEMS devices. In addition, the Architect is a mixed circuit simulator that consists of Schematic capture engine, schematic symbolic library, timing waveform analyzer, layout generator, plus standard elements that feature parameterized Electromechanical, Optical, Hydraulic, Electronics, Magnetic, Thermal, Automotive, Digital and Fluidics behavioral models. Also it has inbuilt component libraries from different companies.

3.4.2 Designer

The Designer is used as a design creation tool, which is specifically suitable for MEMS layout. Further, there are three practical building blocks that the designer consists of: a 2D layout editor, a geometry editor and material property database, and a 3D preprocessor. The geometry editor and material property database, which Architect and Analyzer can use and update, serves as a repository for all of the information necessary for building manufacturing processes for a device. Additionally, Coventor provides default Material Properties Database (MPD) with the software. However, all of the materials, which are commonly used for MEMS processes are included in this file along with significant electrical, mechanical, fluidic, thermal and other generic material property values. The Material Properties Database (MPD) is used as a source for materials in the Process Editor when identifying the steps of the deposition. Figure (15) shows the function manager window for the Designer.

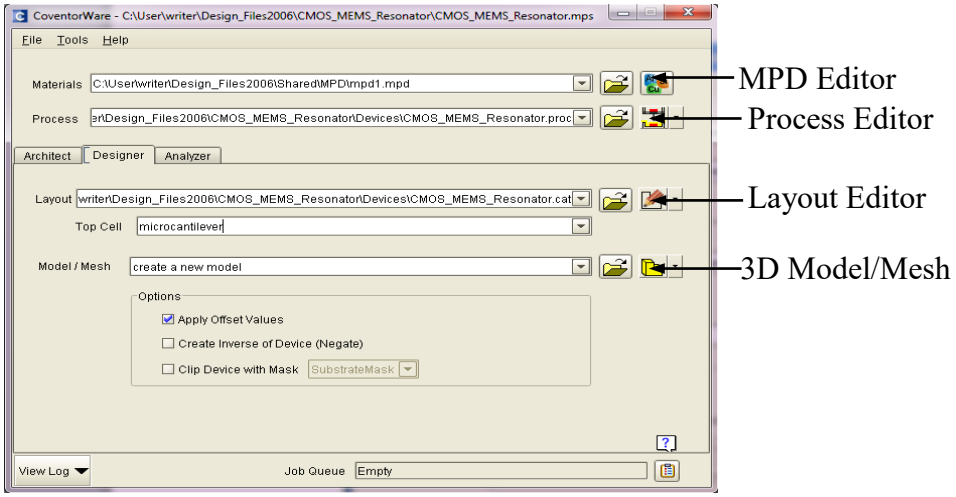

Figure 15 Function manager for the Designer

While, the Process Editor provides a way of creating or editing a description of the fabrication process, which is stored in the process file. The process file provides the process information needed to create a 3-D model. An actual wafer fabrication process can be represented by a series of deposit and etch steps. This specification, along with a 2-D layout, can be used to build a 3-D solid model. Furthermore, the Process Editor consists of three main components, which they are Process Library, Process Description and Step parameters as shown in Figure (16).

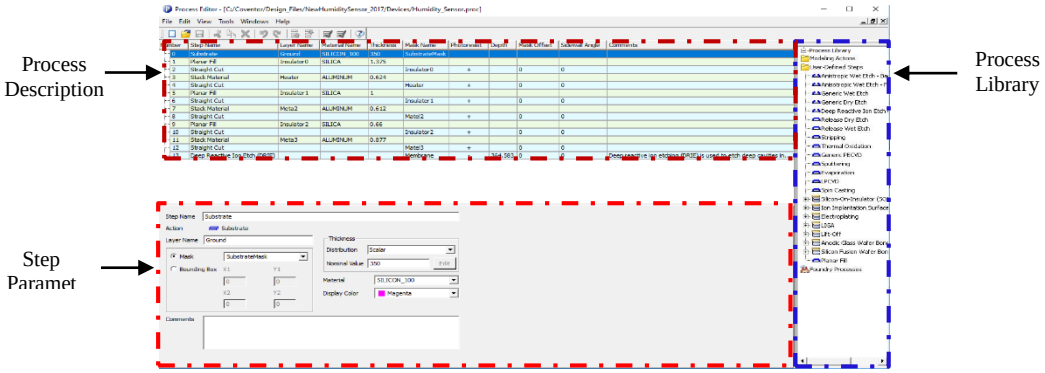

Figure 16 The Process Editor Window

The 2-D Layout Editor provides a number of curve creation tools, which has the capability of generating and fitting true curves, as well as a wide variety of polygon creation and editing tools. In addition, the true curve feature permits curved MEMS components to be automatically meshed. However, the Layout Editor can handle both complex and simple designs, with the knack to arrange designs into hierarchical structures, and at the same time to push down editing to any chosen level in the hierarchy. Figure (17) shows the 2-D design of the device.

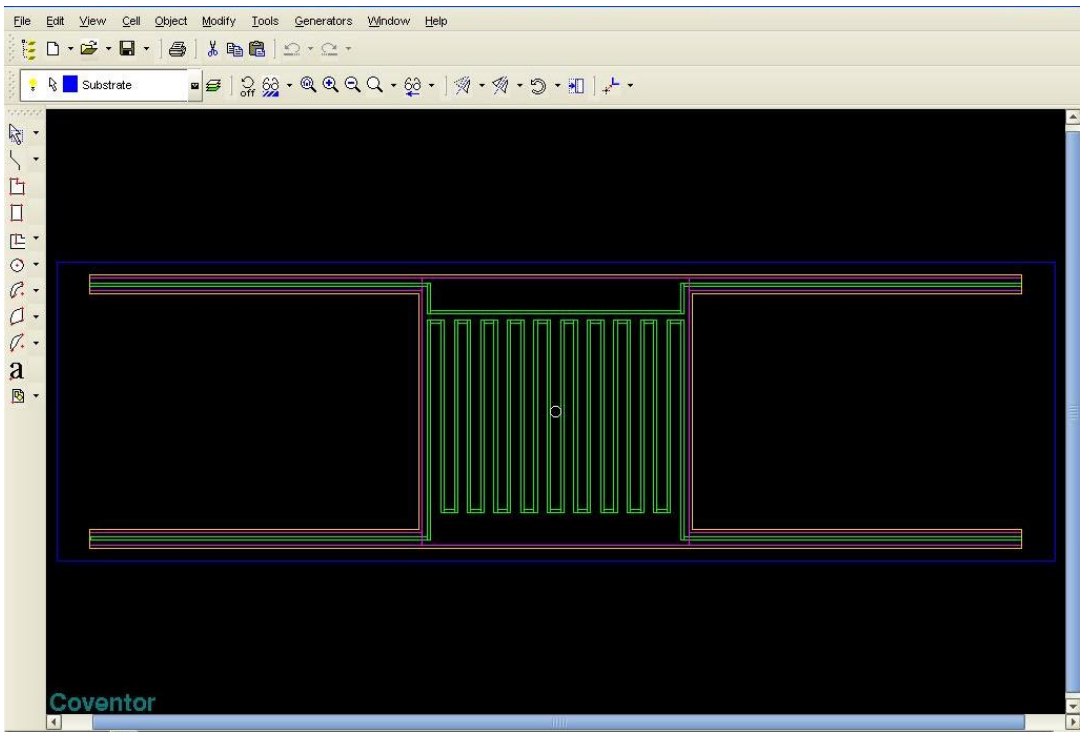

Figure 17 The 2-D design of the CMOS-MEMS Resonator using the Layout Editor

A solid model of a MEMS or a microfluidics device can be produced by the solid modeling tool, which can be done by applying the process description to a 2-D layout. Each deposit layer in the process file corresponds to a layer in the Solid Model folder. The model acts as a verification that the fabrication process will produce a device with the desired 3-D geometry as shown in Figure (17). The model must now be meshed as the next step, to reduce geometry structure into groups in order to create simpler finite element brick, surface or tetrahedral meshing to be presented to the solver for finite element analysis. Further, the solid model tool uses the 2-D layout and process characterization information to build a solid model. Once the 3-D model is created, the next step in physical design is mesh generation. CoventorWare uses finite element and boundary element techniques for solving the differential equations of each physical domain in the problem. The differential equations are solved by discretizing the 3-D model into a mesh, which consists of a number of elements, each with a specified number of nodes as shown in Figure (18).

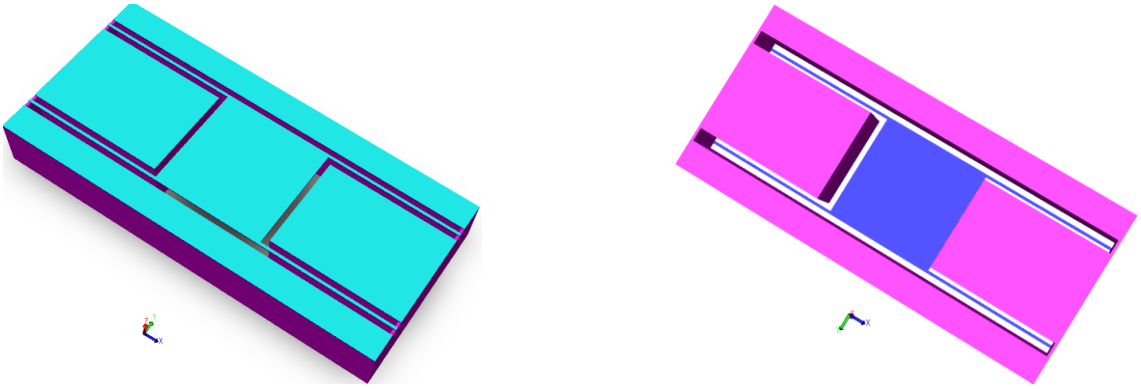

(a) (b)

Figure 18 The 3-D solid model of the CMOS-MEMS Resonator showing (a) front side view and (b) backside view

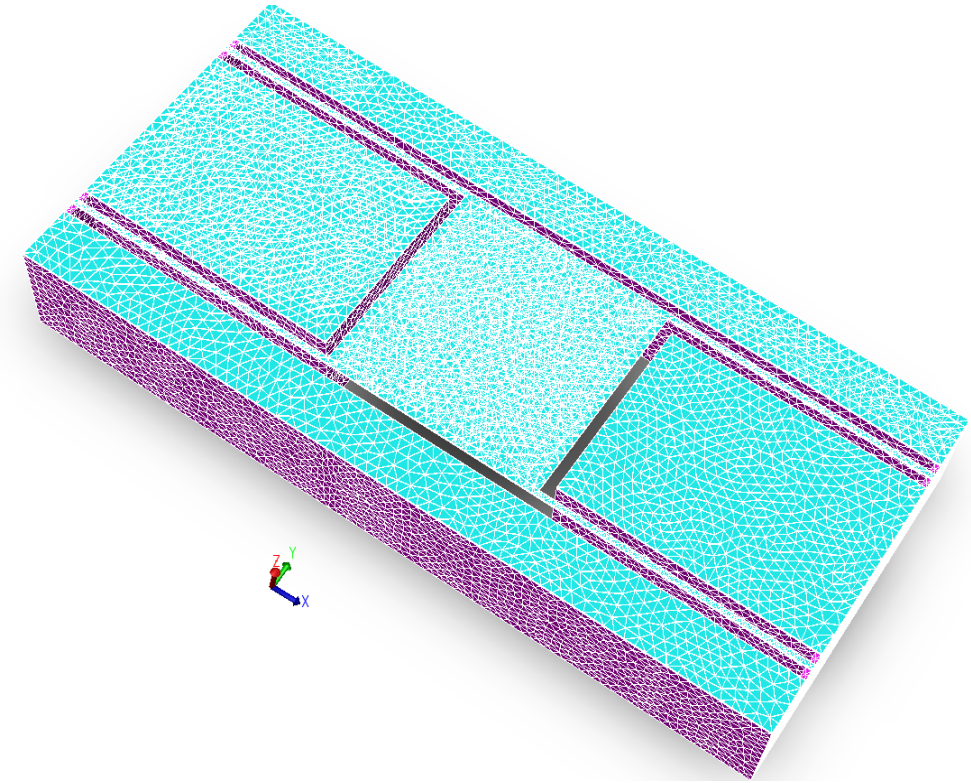

Figure 19 The Meshed 3-D solid model of the multi-layered CMOS-MEMS Resonator

3.4.3 Analyzer

Analyzer is coventor's extensive suite of premiere analysis tools designed specifically for MEMS applications. Analyzer gives the ability to analyze and simulate the behavior of MEMS devices that are subjected to multiple physical forces. Analyzer works hand-in-hand with CoventorWare Designer to provide a manufacturing-aware design flow. A sophisticated Preprocessor serves as the bridge between the tools - users can view 3D models created in designer and then easily prepare them for simulation using automated meshing capabilities that have been optimized for MEMS and microfluidics geometries. Further, the numerical methods underlying Analyzer's solvers includes Finite Element Method (FEM), optimal for structural mechanics. A modal analysis calculation computes the natural resonant frequencies of a mechanical structure at equilibrium. At these resonant frequencies, an undamped (lossless) mechanical structure responds to abounded excitation with an unbounded response. Figure (20) shows the Analyzer Window, which allows the user to access the solver and run the simulation.

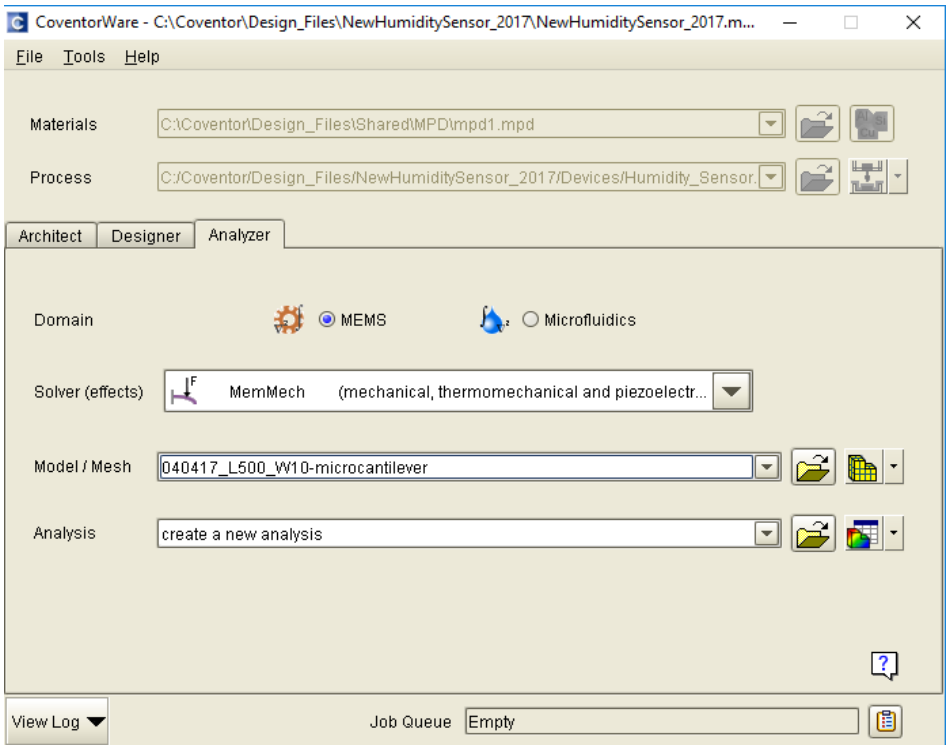

Figure 20 The Analyzer Window

An access to dialogs that set the boundary conditions for the MemMech solver is provided by the hierarchical MemMech BCs window as shown in figure (21). Furthermore, the harmonic analysis is constructed MemMech. The software computes a displacement solution based on a user range of input harmonic frequencies. MemMech runs a modal analysis as part of the harmonic analysis because the solution includes the computation of the model's natural frequencies.

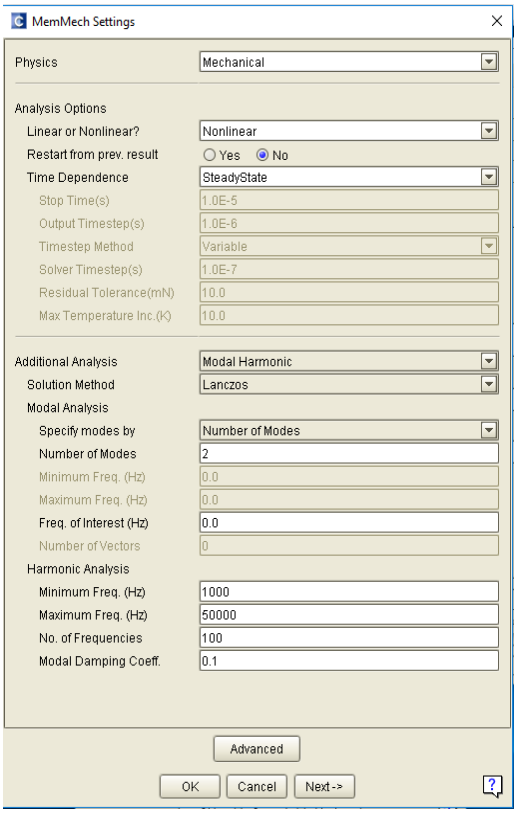

Figure 21 MemMech settings Window

The MemMech BCs dialogs allow the user to set the mechanical boundary conditions for the solver. Patches may be fixed in 3-D space, pressure loads and temperatures may be applied, air flow may be set for convection analysis, boundary conditions may be applied to entire volumes, filter parameters can be set, and special boundary conditions for harmonic analysis can be selected as shown in Figure (22).

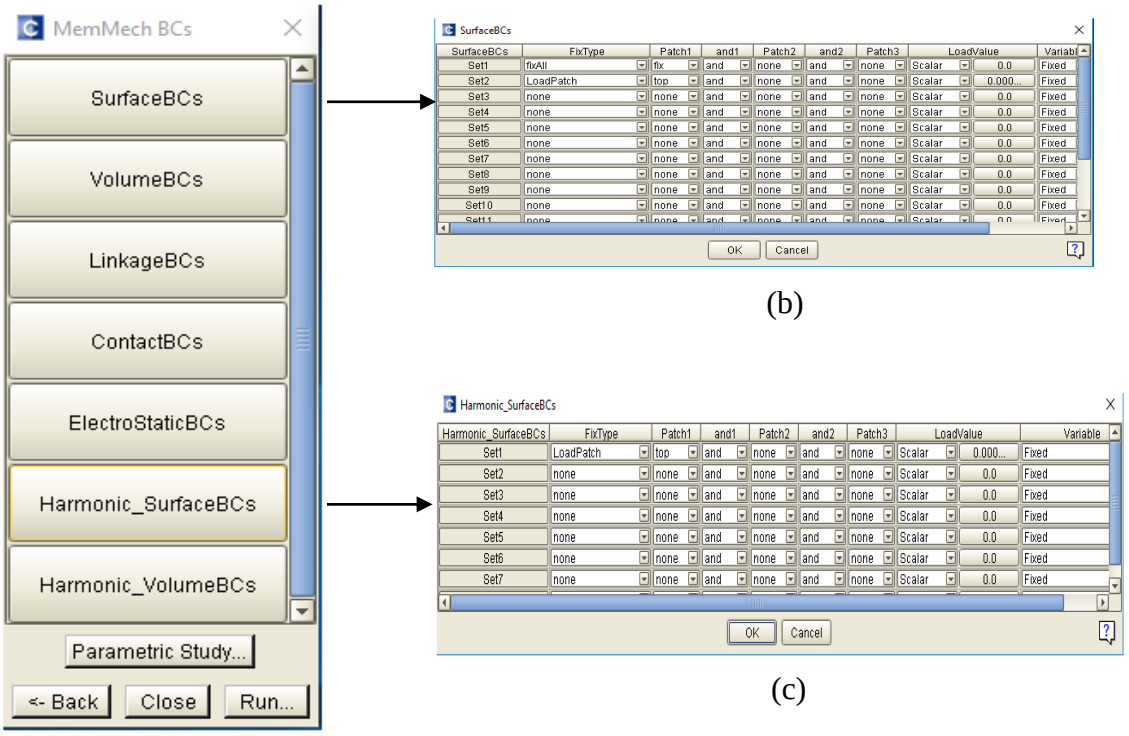

(a)

(b)

(c)

Figure 22 MemMech BCs, (b) surface BCs and (c) harmonic surface BCs

3.5 Summary

This chapter describes the methodology used in this project. The chapter firstly gives overview of the research methodology and described the design parameters of the CMOS-MEMS resonator. This is followed by the theoretical model and mechanical behavior of the resonator. This includes the spring constant of the device, its mass, squeeze film damping, resonance frequency and *Q* factor. Lastly, CoventorWare simulation software is used to design the device following 0.35 µm CMOS technology design rules and post-CMOS micromachining to verify theoretical results using FEA simulation.

Chapter 4

Results and Discussion

The theoretical concepts of the CMOS-MEMS device are developed using proper principles of electromechanical vibrations as explained in section 3.3. The theoretical results of the device parameter are obtained and discussed. The parameters of CMOS-MEMS resonator (spring constant, total mass, natural frequency, squeeze film damping, damping coefficient, damping ratio and *Q* factor), theoretically are obtained based on analytical modeled equations. FEA simulation is used to verify theoretical results.

4.1 Theoretical Results of the CMOS-MEMS Resonator

The overall spring constant is calculated by using Eq. (1) for different lengths and widths as shown in Table 7 and Figure (23).

Table 7 Spring constant at different lengths and widths of the beam

Length (µm)	**Spring constant (N/m)**				
	Width (µm)				
	10	**12**	**14**	**16**	**18**
300	14.5	17.4	20.3	23.2	26.1
350	9.1	11.0	12.8	14.6	16.4
400	6.1	7.3	8.6	9.8	11.0
450	4.3	5.2	6.0	6.9	7.7
500	3.1	3.8	4.4	5.0	5.6

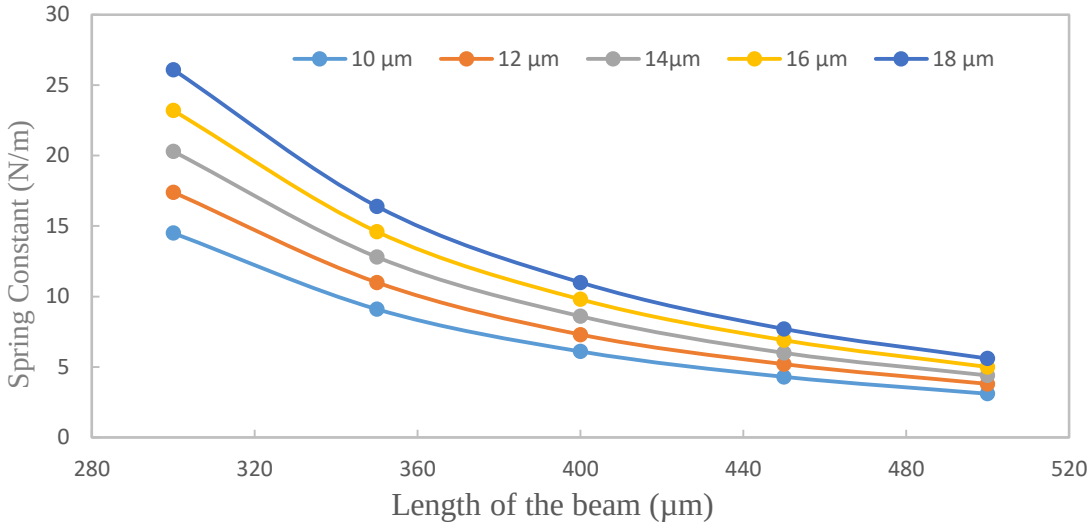

Figure 23 Spring Constant of the Resonator for different lengths and widths

It is observed that the spring constant decreases with increasing the length of the beams from 300 µm to 500 µm. Also, it is observed that the spring constant increases with increasing the width of the beams from 10 µm to 18 µm.

Eq. (3) to Eq. (6) are used to calculate the total mass of the resonator and Eq. (7) is used to calculate the natural frequency without damping. Table 8 and Figure (24) shows the resonance frequency of the resonator at variation in lengths of the beam from 300 µm to 500 µm and variation in width of the beam from 10 µm to 18 µm.

Table 8 Resonance frequency at different lengths and widths

Length (µm)	**Resonance frequency (kHz)**				
	Width (µm)				
	10	**12**	**14**	**16**	**18**
300	12.641	13.813	14.884	15.873	16.795
350	10.011	10.935	11.778	12.555	13.280
400	8.177	8.928	9.613	10.244	10.830
450	6.839	7.464	8.033	8.557	9.044
500	5.827	6.358	6.840	7.283	7.695

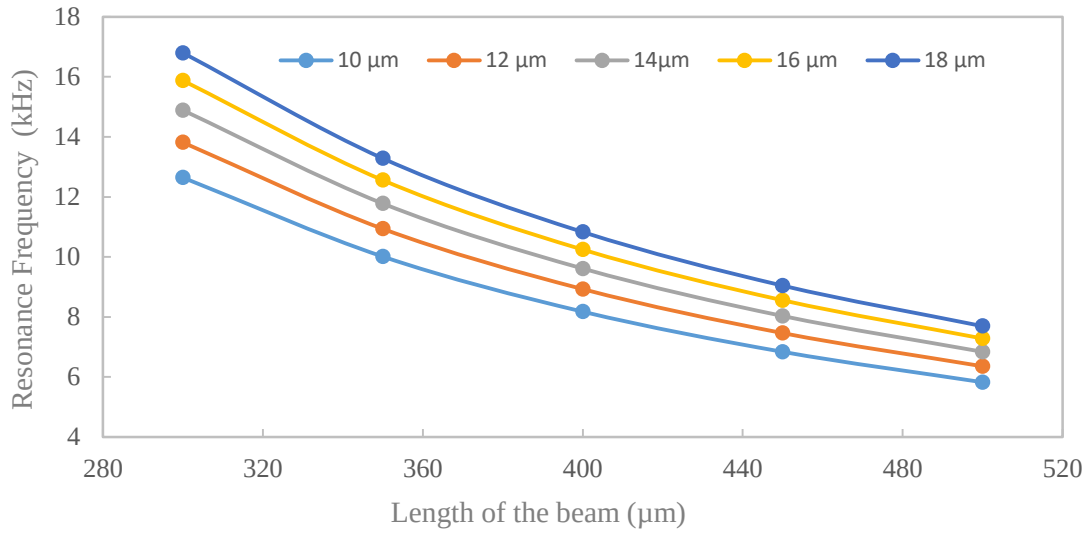

Figure 24 Resonance Frequency for different lengths and widths

We can see the frequency decreases with increasing the length of the beam from 300 µm to 500 µm, while frequency increases with increasing the width of the beam from 10 µm to 18 µm. The air damping of the beam due to the interaction of the vibrating micro-plate with air trapped air in the air gap is calculated using Eq. (10). The damping ratio influences the dynamics of the structure. Figure (25) shows the squeeze film damping of the resonator as function of air gap increases when the length and width of the beam 500 µm and 10 µm, respectively. Consequently, the damping effect can be neglected since the frequency unaffected by the increase in the damping coefficient.

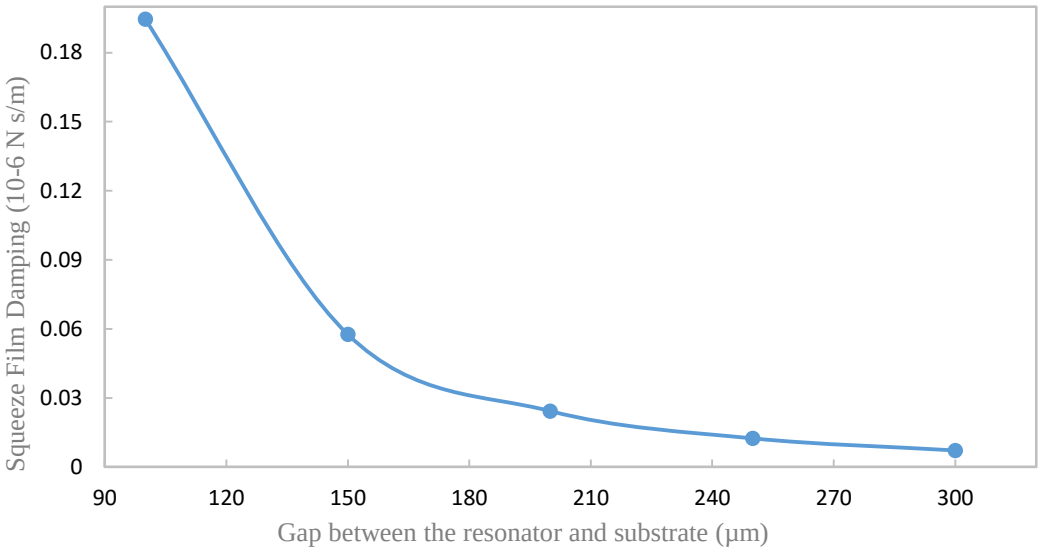

Figure 25 Squeeze film damping of the resonator vs. the air gap between the resonator and substrate

It is theoretically observed that the squeeze film damping decreases from 0.194×10^{-6} N s/m to 7.2×10^{-9} N s/m with increases in gap distance between the resonator and substrate from 100 µm to 300 µm. While, Eq. (12) is used to obtain the *Q* factor under the influence of damping and Figure (26) represents the results of the *Q* factor.

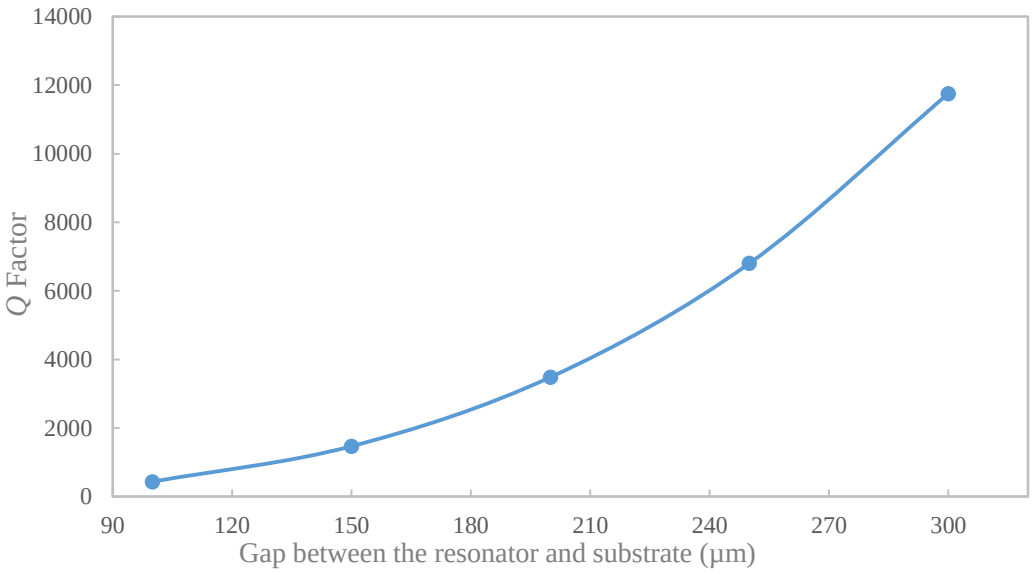

Figure 26 Q factor vs. gap between the resonator and substrate

Due to the relationship between the squeeze film damping and the *Q* factor, it is observed from the figure that by increasing the air gap between the resonator and substrate the *Q* factor increases from 535 *Q* factor to 11756 *Q* factor.

4.2 FEA Simulation Results of the CMOS-MEMS Resonator

CoventorWare is the finite element analysis (FEA) simulation software used to verify the device parameters such as resonant frequency. The simulation results of the analyzer for the beams' length of 500 µm and width of 10 µm is shown in Figure (27), where the maximum normalized plate displacement is 1µm.

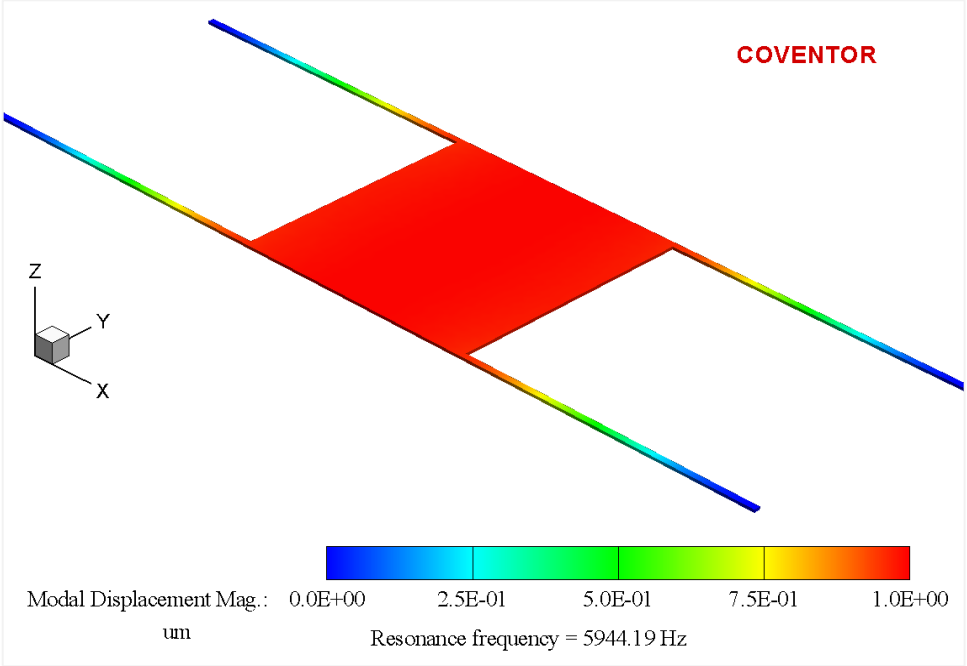

Figure 27 Analyzer results for beams' length and width of 500 µm and 10 µm, respectively

Table 9 and Figure (28) compare the modelled resonance frequency for the 10 µm beams' width with the simulated frequency for the same width versus the beams' length.

Table 9 Modelled and simulated resonance frequencies comparison

Length (µm)	Resonance frequency (kHz)		Error (%)
	10 (µm) Width		
	Modelling	Simulation	
300	12.641	12.92305	2.23
350	10.011	10.43079	4.19
400	8.177	8.542358	4.47
450	6.839	6.914487	1.10
500	5.827	5.944192	2.01

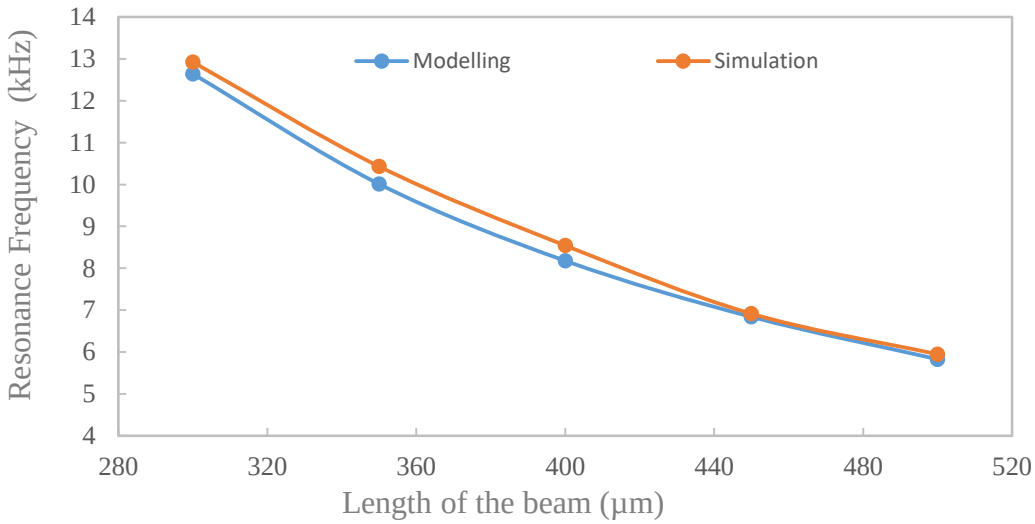

Figure 28 Modelled and simulated resonance frequencies vs beams' length for beam width of 10 µm

As it can be seen the modelled values of the resonance frequency were very close to the simulated values within a percentage error from 1.1% to 4.47%. This matching of the results between modelling and simulation will provide more confidence on the design to be sent for the fabrication.

Chapter 5

Conclusion

In summary, this project focuses on the mathematical modeling and the FEA simulation for the proposed design of a CMOS-MEMS resonator for applications of relative humidity measurement using standard 0.35μm CMOS foundry fabrication technology. The results of mathematical modeling and FEA simulation of a CMOS-MEMS resonator has been presented.

The effect of changes on the lengths and widths of the beam on spring constant and resonant frequency were investigated. The spring constant and resonant frequency decreases with increasing the length of the beam and increases with increasing the width of the beam. Because of varying the length of the beams from 300 μm to 500 μm and the width from 10 μm to 18 μm, it has been found that decreasing the length and increasing the width of the beams will lead to a high spring constant such as 26.1 N/m. Consequently, the higher the spring constant is the higher the frequency due to the proportional relationship between the resonance frequency and the spring constant.

The effect of air damping on the resonant frequency and quality factor were investigated. The damping coefficient was found to decreases from 194×10^{-9} Ns/m to 7.2×10^{-9} Ns/m with increase in the air gap distance between the resonator and substrate from 100 μm to 300 μm. As expected, the *Q* factor decreases from 11765 to 535 with increasing damping coefficient, while the frequency of the CMOS-MEMS resonator remains unaffected. FEA simulation was used to verify the modelled results. The results show good agreement between theoretical and simulation results, with a percentage difference from 1.1% to 4.47 % for resonance frequency.

5.1 Future Work

Time is considered as the only project constraint that a student hold no control of. Even though the mathematical modeling and the simulated results of this research were achieved, the following are recommended for future extensions of the work:

- To investigate the power dissipation for the device.
- To investigate the uniformity of temperature distribution for the device.
- To design the PZR which is used as a transducer for the sensing principle.
- To send the device for fabrication.

References

[1] P. Saffo, "Sensors: the next wave of innovation," *Commun. ACM,* vol. 40, pp. 92-97, 1997.

[2] H. Baltes, O. Brand, A. Hierlemann, D. Lange, and C. Hagleitner, "CMOS MEMS-present and future," in *Micro Electro Mechanical Systems, 2002. The Fifteenth IEEE International Conference on*, 2002, pp. 459-466.

[3] S. Middelhoek, "Quo vadis silicon sensors?," *Sensors and Actuators A: Physical,* vol. 41, pp. 1-8, 4/1/ 1994.

[4] S. S. Li, "CMOS-MEMS resonators and their applications," in *European Frequency and Time Forum & International Frequency Control Symposium (EFTF/IFC), 2013 Joint*, 2013, pp. 915-921.

[5] B. Serban, V. Avramescu, M. Brezeanu, R. Gavrila, A. Dinescu, O. Buiu*, et al.*, "Talc-impregnated polyimide for humidity sensors with improved hysteresis," in *Semiconductor Conference (CAS), 2015 International*, 2015, pp. 109-112.

[6] J.-Q. Huang, F. Li, M. Zhao, and K. Wang, "A Surface Micromachined CMOS MEMS Humidity Sensor," *Micromachines,* vol. 6, p. 1440, 2015.

[7] Z. Yuan, H. Tai, X. Bao, Z. Ye, C. Liu, and Y. Jiang, "Enhancement humidity sensing properties of graphene oxide/Poly(ethyleneimine) film QCM sensors," in *SENSORS, 2015 IEEE*, 2015, pp. 1-4.

[8] J.-O. Dennis, A.-Y. Ahmed, and M.-H. Khir, "Fabrication and Characterization of a CMOS-MEMS Humidity Sensor," *Sensors,* vol. 15, p. 16674, 2015.

[9] R. E. Davis, G. R. McGregor, and K. B. Enfield, "Humidity: A review and primer on atmospheric moisture and human health," *Environmental Research,* vol. 144, Part A, pp. 106-116, 1// 2016.

[10] A. P. Sigumonrong, T. Y. Bong, S. C. Fok, and Y. W. Wong, "Self-learning neurocontroller for maintaining indoor relative humidity," in *Neural Networks, 2001. Proceedings. IJCNN '01. International Joint Conference on*, 2001, pp. 1297-1301 vol.2.

[11] D. Zhang, H. Chang, P. Li, R. Liu, and Q. Xue, "Fabrication and characterization of an ultrasensitive humidity sensor based on metal oxide/graphene hybrid nanocomposite," *Sensors and Actuators B: Chemical,* vol. 225, pp. 233-240, 2016.

[12] X. Wang and M. Ye, "Hysteresis and nonlinearity compensation of relative humidity sensor using support vector machines," *Sensors and Actuators B: Chemical,* vol. 129, pp. 274-284, 1/29/ 2008.

[13] P. Wolkoff and S. K. Kjærgaard, "The dichotomy of relative humidity on indoor air quality," *Environment International,* vol. 33, pp. 850-857, 8// 2007.

[14] A. V. Arundel, E. M. Sterling, J. H. Biggin, and T. D. Sterling, "Indirect health effects of relative humidity in indoor environments," *Environmental Health Perspectives,* vol. 65, p. 351, 1986.

[15] L.-T. Chen, C.-Y. Lee, and W.-H. Cheng, "MEMS-based humidity sensor with integrated temperature compensation mechanism," *Sensors and Actuators A: Physical,* vol. 147, pp. 522-528, 10/3/ 2008.

[16] M. V. Sreelekshmi, S. Gupta, and K. Chidambaram, "Room temperature synthesized nano metal oxide humidity sensor," *International Journal of Applied Engineering Research,* vol. 8, pp. 2361-2363, 2013.

[17] K.-P. Yoo, L.-T. Lim, N.-K. Min, M. J. Lee, C. J. Lee, and C.-W. Park, "Novel resistive-type humidity sensor based on multiwall carbon nanotube/polyimide composite films," *Sensors and Actuators B: Chemical,* vol. 145, pp. 120-125, 3/4/ 2010.

[18] L. Gu, Q.-A. Huang, and M. Qin, "A novel capacitive-type humidity sensor using CMOS fabrication technology," *Sensors and Actuators B: Chemical,* vol. 99, pp. 491-498, 5/1/ 2004.
[19] P.-G. Su and C.-L. Uen, "A resistive-type humidity sensor using composite films prepared from poly(2-acrylamido-2-methylpropane sulfonate) and dispersed organic silicon sol," *Talanta,* vol. 66, pp. 1247-1253, 6/15/ 2005.
[20] P. V. D. Loeppert, IL, US), "Integrated CMOS/MEMS Microphone Die Components," United States Patent, 2016.
[21] G. K. Fedder, R. T. Howe, T. J. K. Liu, and E. P. Quevy, "Technologies for Cofabricating MEMS and Electronics," *Proceedings of the IEEE,* vol. 96, pp. 306-322, 2008.
[22] M. H. Li, C. Y. Chen, C. S. Li, C. H. Chin, and S. S. Li, "A Monolithic CMOS-MEMS Oscillator Based on an Ultra-Low-Power Ovenized Micromechanical Resonator," *Journal of Microelectromechanical Systems,* vol. 24, pp. 360-372, 2015.
[23] Y. K. Liao, C. H. Chiang, and M. S. C. Lu, "Automated Resonance Matching for CMOS MEMS Micro-Resonators," *IEEE Sensors Journal,* vol. 16, pp. 7685-7692, 2016.
[24] M. Gafare, M. H. M. Khir, A. Rabih, A. Ahmed, and J. O. Dennis, "Modeling and simulation of polysilicon piezoresistors in a CMOS-MEMS resonator for mass detection," in *Micro and Nanoelectronics (RSM), 2015 IEEE Regional Symposium on*, 2015, pp. 1-4.
[25] M. Yoichi, "Applications of piezoelectric actuator," *NEC Technical Journal,* vol. 1, pp. 82-86, 2006.
[26] F. Hu, Y. Tang, and Y. Qian, "Design of a MEMS micromirror actuated by electrostatic repulsive force," *Optik - International Journal for Light and Electron Optics,* vol. 123, pp. 387-390, 3// 2012.
[27] J. a. H. Shieh, JE and Fleck, NA and Ashby, MF, "The selection of sensors," *Progress in Materials Science,* vol. 46, pp. 461-504, 2001.
[28] D. S. Eddy and D. R. Sparks, "Application of MEMS technology in automotive sensors and actuators," *Proceedings of the IEEE,* vol. 86, pp. 1747-1755, 1998.
[29] S. W. Harun, M. Yasin, and H. Ahmad, "Micro-displacement sensor with multimode fused coupler and concave mirror," *Laser Physics,* vol. 21, pp. 729-732, 2011.
[30] C. S. Smith, "Piezoresistance Effect in Germanium and Silicon," *Physical Review,* vol. 94, pp. 42-49, 04/01/ 1954.
[31] Y. Kanda, "Piezoresistance effect of silicon," *Sensors and Actuators A: Physical,* vol. 28, pp. 83-91, 1991/07/01 1991.
[32] J. Rausch, P. Heinickel, B. Koegel, K. Zogal, and P. Meissner, "Experimental comparison of piezoresistive MEMS and fiber bragg grating strain sensors," in *2009 IEEE Sensors*, 2009, pp. 1329-1333.
[33] N. C. C. Lu, L. Gerzberg, L. Chih-Yuan, and J. D. Meindl, "Modeling and optimization of monolithic polycrystalline silicon resistors," *IEEE Transactions on Electron Devices,* vol. 28, pp. 818-830, 1981.
[34] O. Yoshiharu and S. Kunihiko, "Piezoresistive Properties of Polycrystalline Silicon Thin Film," *Japanese Journal of Applied Physics,* vol. 11, p. 20, 1972.
[35] G. Schiavone, A. S. Bunting, M. P. Y. Desmulliez, and A. J. Walton, "Fabrication of Electrodeposited Ni–Fe Cantilevers for Magnetic MEMS Switch Applications," *Journal of Microelectromechanical Systems,* vol. 24, pp. 870-879, 2015.
[36] R. Datta, S. Pradhan, and B. Bhattacharya, "Analysis of a seven link robot gripper with an integrated piezoelectric actuation system," in *Control Automation Robotics & Vision (ICARCV), 2014 13th International Conference on*, 2014, pp. 1876-1881.

[37] B. Sviličić, E. Mastropaolo, and R. Cheung, "Widely tunable MEMS ring resonator with electrothermal actuation and piezoelectric sensing for filtering applications," *Sensors and Actuators A: Physical,* vol. 226, pp. 149-153, 5/1/ 2015.
[38] L. Xiuyuan, Z. Yulong, and H. Tengjiang, "Design of a novel electrothermal actuator for integrated MEMS safety-and-arming devices," in *Nano/Micro Engineered and Molecular Systems (NEMS), 2015 IEEE 10th International Conference on*, 2015, pp. 63-66.
[39] V. P. J. Chung, J. K. C. Liang, C. L. Cheng, M. C. Yip, and W. Fang, "Development of a CMOS-MEMS RF-aerogel-based capacitive humidity sensor," in *IEEE SENSORS 2014 Proceedings*, 2014, pp. 190-193.
[40] C.-L. Dai, "A capacitive humidity sensor integrated with micro heater and ring oscillator circuit fabricated by CMOS–MEMS technique," *Sensors and Actuators B: Chemical,* vol. 122, pp. 375-380, 3/26/ 2007.
[41] C. Liu, *Foundations of MEMS*: Prentice Hall Press, 2011.
[42] J. S. Pulskamp, "Modeling, Fabrication, and Testing of a Piezoelectric MEMS Vibrational Energy Reclamation Device," DTIC Document2005.
[43] J. Dennis, A. Ahmed, M. M. Khir, and A. Rabih, "Modelling and Simulation of the Effect of Air Damping on the Frequency and Quality factor of a CMOS-MEMS Resonator," *Appl. Math. Infor. Sci.(AMIS),* vol. 9, pp. 729-737, 2015.
[44] W. Wai-Chi, A. Azid, and B. Y. Majlis, "Formulation of stiffness constant and effective mass for a folded beam," *Archives of Mechanics,* vol. 62, pp. 405-418, 2010.
[45] A. Y. Ahmed, J. O. Dennis, M. H. M. Khir, and M. N. M. Saad, "Analytical modeling of mass-sensitive gas sensor based on MEMS resonator," in *2011 National Postgraduate Conference*, 2011, pp. 1-3.
[46] M. Bao and H. Yang, "Squeeze film air damping in MEMS," *Sensors and Actuators A: Physical,* vol. 136, pp. 3-27, 5/1/ 2007.
[47] M. J. Novack, "Design and fabrication of a thin film micromachined accelerometer," Master of Science in Mechannnnnical Engineering Department of Mechannnnnical Engineering Massachusetts Institute of Technology, Massachusetts Institute of Technology, 1992.
[48] S. Bedair, "Sub-nanogram Mass Loading CMOS-MEMS Cantilever Resonator Oscillators for Gas Detection," Doctor of Philosophy, Carnegie Mellon University, 2008.
[49] A. Rabih, J. Dennis, H. Khir, M. Abdalrahman, and A. Ahmed, "Modelling and Simulation of Polysilicon Piezoresistors in CMOS-MEMS Resonator for Biomarker Detection in Exhaled Breath," in *2015 6th International Conference on Intelligent Systems, Modelling and Simulation*, 2015, pp. 246-251.